END THEORY

The Evans Relational Framework

From ordered change to observable waves
A textbook and working manual for nodes, capacity, fields, geometry, and evidence

Jordan Ryan Evans

Site Edition • 2026

END THEORY

The Evans Relational Framework

From ordered change to observable waves

Jordan Ryan Evans

A dual-path textbook: conceptual reading and technical verification

Publication note

Scientific scope. End Theory is presented here as a research framework. Equations marked **DERIVED** follow from the stated benchmark assumptions. Items marked **DEFINED** fix language or notation. Items marked **PROPOSED** are model choices awaiting a full bridge to observation. Items marked **MEASURED INPUT** enter from metrology or experiment. Items marked **TEST** state a calculation or comparison that can decide a claim.

The author name is set as **Jordan Ryan Evans**; the short form **Ryan Evans** is used in biographical contexts. Historical contributors are credited in the chapter notes and the annotated bibliography.

Edition: 1.0 • 6 August 2026
Prepared in Medicine Hat, Alberta, Canada

How to read this book

This book has two synchronized routes. The first route explains each idea in ordinary language. The second route derives the equation, checks its units, names its inputs, and shows a calculation that can be repeated with pencil, calculator, or code.

FIRST LOOK

If you are ten, begin with the blue boxes and the pictures. A node is a thing that can hold a state. A link says which nodes can affect one another. A wave is a change that travels. A clock is a pattern that repeats. The formal pages then show exactly how those simple sentences become mathematics.

PROOF PATH

If you already know calculus and linear algebra, read Chapters 6–13 in sequence, then use the Concept Atlas as a dependency map. Every displayed result is tagged by status, and every numerical example distinguishes a model output from a measured input or unit definition.

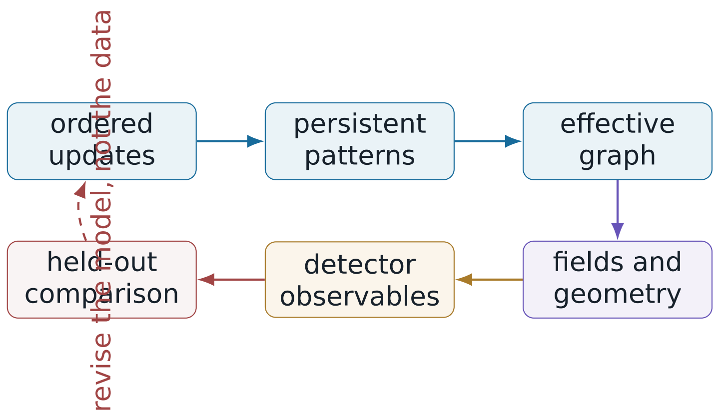

DRY NOTE FROM THE FLIGHT DECK

The universe has declined to sign the reader agreement. It remains free to disagree with every proposed equation. That inconvenience is the point of the test labels.

The claim grammar

Tag	Meaning	What the reader can check
DEFINED	A symbol, convention, identity, or classification is fixed.	Substitute the definitions and check the units or algebra.
DERIVED	The result follows from declared assumptions.	Repeat the variation, proof, series expansion, or numerical test.
PROPOSED	A candidate law or bridge has been selected.	Verify internal consistency, then calculate its distinguishing consequences.
MEASURED INPUT	A value enters from metrology or an empirical fit.	Trace the source, uncertainty, covariance, scale, and unit system.
TEST	A frozen mapping reaches a held-out observable.	Apply the stated likelihood or failure rule without changing the inputs.

Contents

List of Figures

List of Tables

PART I

A universe built from relations

1

Begin without a stage

Newtonian mechanics begins with positions and a time variable; relativity combines space and time into geometry; quantum field theory assigns operators or fields to spacetime points. End Theory asks a prior question: what mathematical structure is sufficient before a physical distance or duration has been established? The proposed answer is an ordered relational history.

Primitive history DEFINED

$$X_0 \prec X_1 \prec X_2 \prec \cdots, \qquad X_n \in \mathcal{X}, \tag{1.1}$$

where X_n is a complete micro-configuration and $\prec$ means "comes before in the update order." The integer n is dimensionless. It orders records; it is not yet a reading in seconds.

The state X_n may contain internal labels, admissible relations, and a rule for local change. It must not quietly contain the metric that the framework later claims to construct. A useful abstract package is

$$\mathcal{P} = (\mathcal{X}, \mathcal{R}, \mathcal{A}, U_p), \tag{1.2}$$

where $\mathcal{R}$ lists direct relations, $\mathcal{A}$ lists admissible changes, and U_p is an update with fixed parameter vector p.

FIRST LOOK

Imagine a flipbook before anyone has drawn a ruler or a clock inside it. The pages have an order. A character can discover duration only by finding something that repeats: a bouncing light pulse, a turning wheel, or a stable oscillation. Page number is order. Clock reading is a property of a repeating pattern.

1.1 Order becomes time through a clock

Let a persistent subsystem K possess a complex clock observable

$$Z_K(X_n) = A_K(X_n)\exp[\mathrm{i}\Theta_K(X_n)]. \tag{1.3}$$

Unwrap the phase so it increases continuously along a stable cycle. The number of completed cycles is

$$N_K(n) = \frac{\text{unwrap}\,\Theta_K(n) - \Theta_K(0)}{2\pi}. \tag{1.4}$$

After one reference period T_K has been fixed, the clock reads

$$t_K(n) = T_K N_K(n). \tag{1.5}$$

This is the first essential distinction of the framework: n counts updates, while t_K is inferred from dynamics.

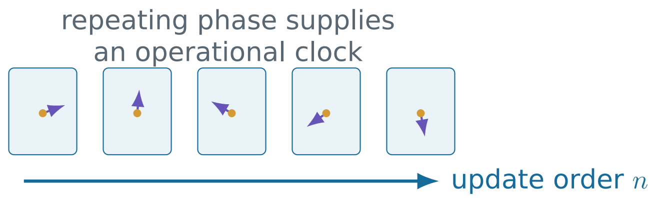

Figure 1.1: The pages advance uniformly in update order, while the internal hand supplies the clock reading.

1.2 When clocks agree

One clock is not yet a universal time coordinate. Suppose two low-load clock types K and L satisfy

$$\frac{t_K(n_2) - t_K(n_1)}{t_L(n_2) - t_L(n_1)} \longrightarrow \gamma_{KL} \tag{1.6}$$

with the same constant γ_{KL} for all sufficiently quiet histories. Then the clocks define compatible duration up to a calibration factor. A relativistic completion must go further: motion and local load must change clock rates universally, not according to the construction details of each clock.

WORK IT OUT

A clock phase advances by 0.40 radians per update. How many updates make one cycle?

$$N = \frac{2\pi}{0.40} = 15.708\ldots$$

Because an update count is an integer, the hand passes one full cycle between updates 15 and 16. If one calibrated cycle is $1\,\mathrm{s}$, then each update corresponds to approximately $1/15.708 = 0.06366\,\mathrm{s}$ in this homogeneous example.

RESEARCH GATE

Construct at least two stable clock patterns from the same update rule. Measure their phase noise, perturbation recovery, and rate ratio. Universal low-energy agreement is the gate from ordered change to physical time.

2

Persistence draws the map

Objects need not be primitive. A flame, a wave crest, and a whirlpool retain recognizable structure while their material constituents change. End Theory uses that familiar idea as a mathematical filter: a candidate object is a pattern that remains equivalent to itself under allowed transport, phase change, or relabeling.

2.1 A test for identity

Choose a coarse-graining map C_R at resolution R, a comparison distance d_R, a group $\mathcal{G}_R$ of allowed transformations, and a tolerance ε_R. A pattern persists for T updates when

$$\inf_{g\in\mathcal{G}_R} d_R(C_R X_{n+T}, gC_R X_n) < \varepsilon_R. \tag{2.1}$$

The corresponding equivalence class is

$$[X]_{R,\varepsilon} = \left\{ Y : \inf_{g\in\mathcal{G}_R} d_R(C_R Y, gC_R X) < \varepsilon_R \right\}. \tag{2.2}$$

The lifetime estimator

$$\tau_R = \inf\{T : d_R(C_R X_{n+T}, \mathcal{G}_R C_R X_n) \geq \varepsilon_R\} \tag{2.3}$$

turns persistence into a number.

FIRST LOOK

You recognize a song even if it is played on another piano. The exact air vibrations differ, but the pattern survives a change of instrument. The transformation group says which differences are allowed; the tolerance says how far the tune may drift before it becomes another tune.

2.2 Influence becomes adjacency

Let a and b label persistent classes. Perturb a by a small admissible change δ and measure the resolved response of b:

$$I_{ab}(n) = \frac{\left\| C_R X^{(a+\delta)}_{n+\Delta} - C_R X_{n+\Delta} \right\|_b}{\|\delta\|}. \tag{2.4}$$

Average over a fixed observation window,

$$w_{ab} = \frac{1}{T}\sum_{n=1}^{T} I_{ab}(n), \tag{2.5}$$

and retain a link when $w_{ab} > w_{\text{min}}$. This constructs an effective weighted graph

$$G_R = (V_R, E_R, W_R). \tag{2.6}$$

The word “local” now has an operational meaning: directly linked patterns respond without an intervening chain.

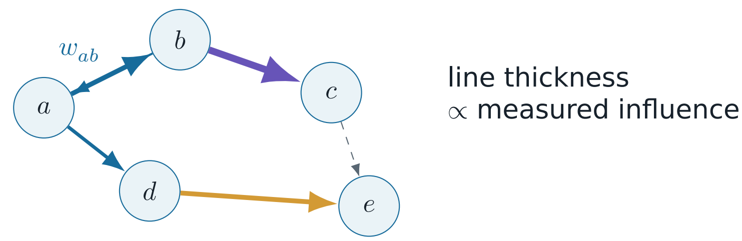

Figure 2.1: The graph is inferred by intervention and response. Direction is permitted until reciprocity is demonstrated.

2.3 Distance and dimension

Assign a positive edge length $\ell_{ab} = \ell_0 f(w_{ab})$ with a declared decreasing function f. The shortest-path distance is

$$d_G(a, b) = \min_{\gamma: a \to b} \sum_{e \in \gamma} \ell_e. \tag{2.7}$$

Dimension can be estimated without first drawing the graph as a cubic lattice. If $\mathsf{L} = D - W$ is its Laplacian, diffusion for parameter σ is generated by

$$K(\sigma) = \exp(-\sigma \mathsf{L}), \qquad P(\sigma) = \frac{1}{|V|} \operatorname{Tr} K(\sigma). \tag{2.8}$$

The scale-dependent spectral dimension is

$$d_s(\sigma) = -2 \frac{\mathrm{d} \ln P(\sigma)}{\mathrm{d} \ln \sigma}. \tag{2.9}$$

For ordinary diffusion in d flat spatial dimensions, $P(\sigma) \propto \sigma^{-d/2}$, so $d_s = d$.

PROOF PATH

Take $P(\sigma) = A\sigma^{-d/2}$. Then $\ln P = \ln A - (d/2) \ln \sigma$. Differentiating with respect to $\ln \sigma$ gives $-d/2$. Multiplying by -2 yields $d_s = d$. No special dimension has been inserted.

DRY NOTE FROM THE FLIGHT DECK

The ratio of a d-ball's volume to its boundary area is $V_d / S_{d-1} = r/d$. It is not unique to three dimensions. A serious dimensional claim therefore comes from dynamical stability and a scale plateau such as Equation (2.9), not from admiring the number three until it confesses.

3

A local capacity for change

The distinctive structural proposal of End Theory is a finite local transition capacity. The constraint is local: each node and its neighbourhood must process a bounded demand during one update. A regional budget is obtained by summing local budgets after the local rule has been applied.

3.1 Demand and residual capacity

For a scalar benchmark, define the local velocity

$$v_i^n = \frac{q_i^{n+1} - q_i^n}{\Delta\tau} \tag{3.1}$$

and an energy-like demand

$$E_i^n = \frac{\mu}{2}(v_i^n)^2 + \frac{\kappa}{4a^2}\sum_{j\sim i} w_{ij}(q_i^n - q_j^n)^2 + V_+(q_i^n), \tag{3.2}$$

where $V_+ \geq 0$ is the portion of the onsite energy assigned to the capacity ledger. With capacity scale $E_\star > 0$,

$$C_i^n = \frac{E_i^n}{E_\star}, \qquad 0 \leq C_i^n \leq 1, \qquad r_i^n = 1 - C_i^n. \tag{3.3}$$

Here r_i^n is residual capacity. It is dimensionless bookkeeping until a coarse-grained physical normalization is supplied.

WORK IT OUT

Take $\mu = 2$, $v = 0.30$, link contribution 0.21, onsite contribution 0.05, and $E_\star = 0.50$ in consistent energy units. Then

$$E = \tfrac{1}{2}(2)(0.30)^2 + 0.21 + 0.05 = 0.35,$$

so $C = 0.35/0.50 = 0.70$ and $r = 0.30$. The calculation is simple on purpose: every later capacity model must reduce to a ledger that a reader can audit term by term.

3.2 From a proposal to an admissible update

Suppose an unconstrained equation proposes $\tilde{q}_i^{n+1}$. Define its proposed increment $\Delta_i = \tilde{q}_i^{n+1} - q_i^n$. A local limiter may be written

$$q_i^{n+1} = q_i^n + \eta_i^n \Delta_i, \qquad 0 \leq \eta_i^n \leq 1, \tag{3.4}$$

with η_i^n chosen from neighbourhood data so that $C_i^n \leq 1$. This is a constructive pattern, not a unique law. A promoted update must satisfy five simultaneous checks:

1. **Closure:** admissible input states map to admissible output states.
2. **Single-valuedness:** every branch and tie-break has one result.
3. **Locality:** the calculation uses a bounded neighbourhood.

4. **Conservation or controlled dissipation:** declared charges obey an exact balance law.
5. **Refinement:** observables converge as the graph and update scale are refined.

The complete capacity-preserving law can be expressed as

$$(X_{n+1}, X_n) = U_p(X_n, X_{n-1}), qquad U_p(\mathcal{A}) \subseteq \mathcal{A}, \tag{3.5}$$

where $\mathcal{A}$ is the capacity-admissible state set.

RESEARCH GATE

Choose a concrete η_i^n. Prove closure by induction, then calculate the discrete energy difference $H^{n+1} - H^n$. A limiter that respects capacity but invents energy has not completed the gate.

Figure 3.1: A visual analogy for local capacity. The overloaded tray changes the robot's local response; the rest of the spacecraft does not need an instantaneous universe-wide inventory. The black hole is off duty and merely provides atmosphere.

4

Patterns can carry physics

In a field theory a particle is associated with an excitation carrying energy, momentum, spin, and charge. In a relational framework the same observable roles must arise from persistent dynamical patterns. The word "particle" is earned by a checklist, not granted to every attractive knot in a simulation.

4.1 The pattern checklist

A candidate pattern P requires:

1. a localized or controlled-support solution;
2. stability under small perturbations;
3. a dispersion relation $E(\mathbf{p})$;
4. conserved or topological labels;
5. a transport rule;
6. scattering or decay amplitudes;
7. a detector-level map.

The first three items can be explored in a scalar benchmark. Charge requires a symmetry and current. Spin requires transformation properties under the emergent rotation or Lorentz group. A familiar mass label can be assigned only after operational energy, momentum, and clock units have been built.

FIRST LOOK

A particle may be more like a travelling stadium wave than a marble. People sit down and stand up; the wave moves around the stadium. The moving pattern is real even though no one person travels with it. The difficult physics begins when the pattern must also carry exact labels, collide predictably, and survive noise.

4.2 A two-node example

Two identical coupled coordinates provide the smallest transparent pattern calculation:

$$\mu\ddot{q}_1 + \mu\Omega_0^2 q_1 + \kappa(q_1 - q_2) = 0, \tag{4.1}$$

$$\mu\ddot{q}_2 + \mu\Omega_0^2 q_2 + \kappa(q_2 - q_1) = 0. \tag{4.2}$$

Introduce normal coordinates

$$q_+ = \frac{q_1 + q_2}{\sqrt{2}}, \qquad q_- = \frac{q_1 - q_2}{\sqrt{2}}. \tag{4.3}$$

Adding and subtracting the equations gives

$$\ddot{q}_+ + \Omega_0^2 q_+ = 0, \tag{4.4}$$

$$\ddot{q}_- + \left(\Omega_0^2 + \frac{2\kappa}{\mu}\right) q_- = 0. \tag{4.5}$$

Thus the collective frequencies are

$$\omega_+ = \Omega_0, \qquad \omega_- = \sqrt{\Omega_0^2 + \frac{2\kappa}{\mu}}. \tag{4.6}$$

The in-phase mode does not stretch the link; the out-of-phase mode does. This is the seed of band structure on a larger graph.

WORK IT OUT

Let $\Omega_0 = 2$, $\kappa = 3$, and $\mu = 6$ in consistent units. Then

$$\omega_+ = 2, \qquad \omega_- = \sqrt{4+1} = \sqrt{5} \approx 2.236.$$

Substitute $q_1 = A\cos(2t)$ and $q_2 = A\cos(2t)$ into the original equations: the link terms cancel. Substitute $q_1 = A\cos(\sqrt{5}t)$ and $q_2 = -q_1$: each link term contributes $2\kappa q_1$, producing the second frequency.

4.3 Wave, bound pattern, and observation

Three levels should remain distinct:

$$\text{micro-state trajectory} \longrightarrow \text{persistent pattern class} \longrightarrow \text{detector record.} \tag{4.7}$$

A wave observation theory specifies every arrow. A detector need not reveal a microscopic node; it responds to coarse conserved quantities and calibrated transfer functions. Chapters 19 and 23 turn this statement into a manual.

5

The logical succession of End Theory

The framework is organized as a dependency chain. Later objects may not be used to define earlier ones. This prevents physical metres, seconds, particle masses, or observed couplings from reappearing as unexplained ingredients in the foundational layer.

5.1 Eight foundational statements

1. **Relational proto-state.** The initial description supplies states, admissible relations, and local changes rather than a prior physical spacetime.
2. **Ordered updates.** Equation (1.1) precedes metric duration.
3. **Operational clocks.** Persistent recurrent patterns define readings by Equation (1.5).
4. **Persistent identity.** Objects are equivalence classes satisfying Equation (2.1).
5. **Emergent adjacency.** A stable influence pattern defines the weighted graph in Equation (2.6).
6. **Local capacity.** Every neighbourhood satisfies Equation (3.3).
7. **Deterministic evolution.** One fixed map of the form (3.5) advances admissible states.
8. **Observable completion.** Preparation, evolution, coarse-graining, and measurement maps determine empirical probabilities and detector records.

5.2 The evidence ladder

Let a model specification be

$$\mathcal{M} = (\mathcal{X}, U_p, B, C_R, \mathcal{O}, \Pi), \tag{5.1}$$

where B denotes boundary/initial conditions, C_R the coarse-graining, $\mathcal{O}$ the observable map, and Π the parameter and calibration policy. A quantity Q has different status depending on how it is obtained:

$$Q \equiv f(\text{definitions}) \qquad \text{identity,} \tag{5.2}$$

$$Q = F_Q(\mathcal{M}) \qquad \text{internal result,} \tag{5.3}$$

$$p \leftarrow D_{\text{cal}} \qquad \text{calibration,} \tag{5.4}$$

$$Q_{\text{test}} = F_Q(\mathcal{M}_{\text{frozen}}) \qquad \text{prediction.} \tag{5.5}$$

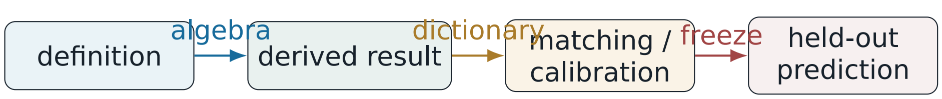

Figure 5.1: A claim advances only by an explicit operation. Reproducing a calibration target is not counted again as a prediction.

5.3 The canonical benchmark

The book now introduces a calculable graph-field benchmark. It supplies an action, an explicit deterministic update, an exact normal-mode spectrum, a stability boundary, and exact finite-spacing Abelian gauge invariance. These results establish the mathematical laboratory in which the broader relational ideas can be tested.

DRY NOTE FROM THE FLIGHT DECK

A grand title does not exempt an equation from arithmetic. In this book, even the universe has to show its working.

PART II

The mathematical engine

6

The small toolkit that carries the theory

The derivations in this book use four recurring operations: finite differences, matrix eigenmodes, variations of an action, and series expansions. This chapter places them in one toolbox so the later equations can be checked rather than merely admired.

6.1 From change to derivative

For a smooth function $q(t)$, Taylor's theorem gives

$$q(t+h) = q + h\dot{q} + \frac{h^2}{2}\ddot{q} + \frac{h^3}{6}q^{(3)} + \frac{h^4}{24}q^{(4)} + \mathcal{O}(h^5), \tag{6.1}$$

$$q(t-h) = q - h\dot{q} + \frac{h^2}{2}\ddot{q} - \frac{h^3}{6}q^{(3)} + \frac{h^4}{24}q^{(4)} + \mathcal{O}(h^5). \tag{6.2}$$

Subtracting gives a centred first derivative,

$$\dot{q}(t) = \frac{q(t+h) - q(t-h)}{2h} + \mathcal{O}(h^2), \tag{6.3}$$

while adding and rearranging gives the centred second derivative,

$$\ddot{q}(t) = \frac{q(t+h) - 2q(t) + q(t-h)}{h^2} + \mathcal{O}(h^2). \tag{6.4}$$

FIRST LOOK

Speed asks, "How much did the position change per tick?" Acceleration asks, "How much did the speed change per tick?" Equation (6.4) compares the present value with both neighbours in time, so straight motion cancels and curvature remains.

6.2 Dimensions before numbers

Write $[Q]$ for the dimensions of Q. An equation is dimensionally admissible only if every term being added has the same dimensions. If

$$\mu\ddot{q} + Kq = 0, \tag{6.5}$$

then $[K/\mu] = T^{-2}$. The angular frequency $\omega = \sqrt{K/\mu}$ has dimensions T^{-1}.

For a monomial

$$Q = \prod_{j=1}^{N} x_j^{a_j}, \tag{6.6}$$

the dimension vector of Q is the matrix product of the input-dimension matrix and the exponent vector $\mathbf{a}$. This linear-algebra view is the quickest way to expose a missing metre, second, kelvin, or charge unit.

WORK IT OUT

Check $\ell_P = \sqrt{\hbar G/c^3}$. Using $[\hbar] = ML^2T^{-1}$, $[G] = L^3M^{-1}T^{-2}$, and $[c] = LT^{-1}$,

$$\left[\frac{\hbar G}{c^3}\right] = \frac{(ML^2T^{-1})(L^3M^{-1}T^{-2})}{L^3T^{-3}} = L^2.$$

The square root therefore has dimension L.

6.3 Eigenmodes

For a real symmetric matrix A, the spectral theorem supplies orthonormal eigenvectors $u^{(r)}$ and real eigenvalues λ_r:

$$Au^{(r)} = \lambda_r u^{(r)}. \tag{6.7}$$

Expand $q = \sum_r Q_r u^{(r)}$. The coupled equation

$$\ddot{q} + Aq = 0 \tag{6.8}$$

becomes independent oscillators

$$\ddot{Q}_r + \lambda_r Q_r = 0. \tag{6.9}$$

The graph Laplacian will play the role of A for spatial coupling.

6.4 Varying an action

Let $S[q] = \int L(q, \dot{q}, t)\,\mathrm{d}t$. Perturb the path, $q \mapsto q + \epsilon\eta$, with η vanishing at the endpoints. To first order,

$$\begin{aligned}
\delta S &= \frac{\mathrm{d}}{\mathrm{d}\epsilon} S[q + \epsilon\eta]\Big|_{\epsilon=0} && (6.10)\\
&= \int \left(\frac{\partial L}{\partial q}\eta + \frac{\partial L}{\partial \dot{q}}\dot{\eta}\right)\,\mathrm{d}t && (6.11)\\
&= \int \left[\frac{\partial L}{\partial q} - \frac{\mathrm{d}}{\mathrm{d}t}\left(\frac{\partial L}{\partial \dot{q}}\right)\right]\eta\,\mathrm{d}t. && (6.12)
\end{aligned}$$

Because η is arbitrary,

$$\frac{\mathrm{d}}{\mathrm{d}t}\left(\frac{\partial L}{\partial \dot{q}}\right) - \frac{\partial L}{\partial q} = 0. \tag{6.13}$$

The discrete calculation in Chapter 8 repeats this logic with sums and neighbouring time slices.

7

Graphs, links, and the Laplacian

Let $G = (V, E, W)$ be a finite weighted graph with symmetric nonnegative weights $w_{ij} = w_{ji}$. Its degree matrix and adjacency matrix are

$$D_{ii} = \sum_j w_{ij}, \qquad W_{ij} = w_{ij}. \tag{7.1}$$

The weighted graph Laplacian is

$$\mathsf{L} = D - W, \qquad (\mathsf{L}q)_i = \sum_j w_{ij}(q_i - q_j). \tag{7.2}$$

7.1 Why it behaves like curvature

The quadratic link energy is

$$q^{\mathsf{T}}\mathsf{L}q = \frac{1}{2}\sum_{i,j} w_{ij}(q_i - q_j)^2 \geq 0. \tag{7.3}$$

To verify the identity, expand the square:

$$\frac{1}{2}\sum_{ij} w_{ij}(q_i - q_j)^2 = \frac{1}{2}\sum_{ij} w_{ij}(q_i^2 + q_j^2 - 2q_iq_j) \tag{7.4}$$

$$= \sum_i \left(\sum_j w_{ij}\right) q_i^2 - \sum_{ij} w_{ij}q_iq_j \tag{7.5}$$

$$= q^{\mathsf{T}}(D - W)q. \tag{7.6}$$

Hence all eigenvalues of L are nonnegative. For a connected graph, the constant vector is the unique zero mode.

FIRST LOOK

Put the same number on every node. Every difference $q_i - q_j$ is zero, so the Laplacian sees no bend. Put a bump on one node, and the differences point away from the bump. The Laplacian measures how different a node is from its neighbours.

7.2 A periodic chain

On a one-dimensional chain with spacing a and unit weights,

$$(\mathsf{L}q)_j = 2q_j - q_{j+1} - q_{j-1}. \tag{7.7}$$

For the plane wave $q_j = \exp(ikja)$,

$$(\mathsf{L}q)_j = \left(2 - \mathrm{e}^{ika} - \mathrm{e}^{-ika}\right) q_j \tag{7.8}$$

$$= 4\sin^2\left(\frac{ka}{2}\right) q_j. \tag{7.9}$$

Thus

$$\lambda(k) = 4\sin^2\left(\frac{ka}{2}\right). \tag{7.10}$$

In d hypercubic dimensions,

$$\lambda(\mathbf{k}) = 4\sum_{r=1}^{d}\sin^2\left(\frac{k_r a}{2}\right). \tag{7.11}$$

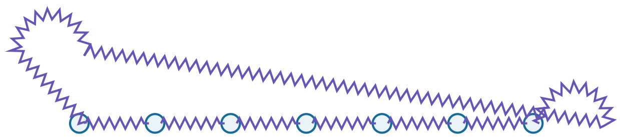

periodic chain: the last node links back to the first

Figure 7.1: A regular benchmark graph. The periodic boundary removes edge effects and makes plane waves exact eigenmodes.

8

The discrete action and update

Fix a graph during a stabilized phase. Let q_i^n be a real coordinate at node i and update n. The benchmark action is

$$\boxed{S_d = \sum_n \Delta\tau \left[\frac{\mu}{2} \sum_i \left(\frac{q_i^{n+1} - q_i^n}{\Delta\tau} \right)^2 - \frac{\kappa}{2a^2} \sum_{\langle ij \rangle} w_{ij} (q_i^n - q_j^n)^2 - \sum_i V(q_i^n) \right].} \tag{8.1}$$

Here $\mu > 0$ is an inertia, $\kappa > 0$ a link stiffness, a a stabilized link scale, and $\Delta\tau$ a benchmark clock step.

8.1 Variation one line at a time

Only the $n-1$ and n kinetic terms contain q_i^n. Their derivative is

$$\frac{\mu}{\Delta\tau} \left[(q_i^n - q_i^{n-1}) - (q_i^{n+1} - q_i^n) \right]. \tag{8.2}$$

The link term contributes

$$-\Delta\tau \frac{\kappa}{a^2} (\mathsf{L} q^n)_i, \tag{8.3}$$

and the onsite term contributes $-\Delta\tau V'(q_i^n)$. Setting the full derivative to zero and dividing by $\Delta\tau$ yields

$$\mu \frac{q_i^{n+1} - 2q_i^n + q_i^{n-1}}{\Delta\tau^2} = -\frac{\kappa}{a^2} (\mathsf{L} q^n)_i - V'(q_i^n). \tag{8.4}$$

Solving for the next state gives the explicit update

$$\boxed{q_i^{n+1} = 2q_i^n - q_i^{n-1} - \frac{\Delta\tau^2}{\mu} \left[\frac{\kappa}{a^2} (\mathsf{L} q^n)_i + V'(q_i^n) \right].} \tag{8.5}$$

PROOF PATH

For a finite graph and differentiable V, every term on the right side of Equation (8.5) is a single real number determined by (q^{n-1}, q^n). Therefore the benchmark recursion is algebraically deterministic. This statement concerns the benchmark update; a capacity projection is a separately declared layer.

8.2 A hand calculation on three nodes

Take a three-node path $1 - 2 - 3$ with unit weights, $\mu = \kappa = a = 1$, $\Delta\tau = 0.1$, and $V = 0$. Let

$$q^{n-1} = (0, 0, 0), \qquad q^n = (0, 1, 0). \tag{8.6}$$

The Laplacian is

$$\mathsf{L} = \begin{pmatrix} 1 & -1 & 0 \\ -1 & 2 & -1 \\ 0 & -1 & 1 \end{pmatrix}, \qquad \mathsf{L} q^n = (-1, 2, -1). \tag{8.7}$$

Equation (8.5) gives

$$q^{n+1} = 2(0,1,0) - (0,0,0) - 0.01(-1,2,-1) \tag{8.8}$$
$$= (0.01, 1.98, 0.01). \tag{8.9}$$

The peak begins to spread to its neighbours. With zero initial velocity, the chosen pair (q^{n-1}, q^n) actually contains a sudden displacement, so the centre also continues forward before the restoring force reverses it.

8.3 An exact discrete invariant in the linear sector

Let $V(q) = \mu\Omega_0^2 q^2/2$ and define the symmetric positive matrix

$$A = \Omega_0^2 I + \frac{\kappa}{\mu a^2}\mathsf{L}. \tag{8.10}$$

The linear update is

$$q^{n+1} - 2q^n + q^{n-1} + \Delta\tau^2 A q^n = 0. \tag{8.11}$$

It preserves

$$H^{n+1/2} = \frac{1}{2}\left\|\frac{q^{n+1} - q^n}{\Delta\tau}\right\|^2 + \frac{1}{2}(q^{n+1})^{\mathsf{T}} A q^n. \tag{8.12}$$

Subtract $H^{n-1/2}$, factor $q^{n+1} - q^{n-1}$, and insert the update; the result is zero. Positivity of this invariant is tied to the stability condition derived in Chapter 10.

9

Exact lattice waves

Use the harmonic onsite potential $V(q) = \mu\Omega_0^2 q^2/2$ on a periodic d-dimensional cubic lattice. Insert the plane wave

$$q_{\mathbf{j}}^{\,n} = A\exp\left[\mathrm{i}(\mathbf{k}\cdot\mathbf{x}_{\mathbf{j}} - \omega n\Delta\tau)\right] \tag{9.1}$$

into Equation (8.4).

9.1 Temporal factor

The centred second difference contributes

$$q^{n+1} - 2q^n + q^{n-1} = \left(\mathrm{e}^{-\mathrm{i}\omega\Delta\tau} - 2 + \mathrm{e}^{\mathrm{i}\omega\Delta\tau}\right) q^n \tag{9.2}$$

$$= -4\sin^2\left(\frac{\omega\Delta\tau}{2}\right) q^n. \tag{9.3}$$

9.2 Spatial factor

Equation (7.11) supplies the spatial eigenvalue. With

$$c^2 \equiv \frac{\kappa}{\mu}, \tag{9.4}$$

the exact lattice dispersion relation is

$$\boxed{\frac{4}{\Delta\tau^2}\sin^2\left(\frac{\omega\Delta\tau}{2}\right) = \Omega_0^2 + \frac{4c^2}{a^2}\sum_{r=1}^{d}\sin^2\left(\frac{k_r a}{2}\right).} \tag{9.5}$$

This is an exact internal result for the declared linear benchmark.

WORK IT OUT

In one dimension take $a = 1$, $\Delta\tau = 0.5$, $c = 1$, $\Omega_0 = 0$, and $k = \pi/3$. The right side is

$$4\sin^2(\pi/6) = 1.$$

Therefore $16\sin^2(\omega/4) = 1$, so $\sin(\omega/4) = 1/4$ and

$$\omega = 4\arcsin(1/4) \approx 1.01072.$$

The continuum value would be $ck = 1.04720$; the lattice mode is slightly lower because finite spacing bends the band.

9.3 The long-wave expansion

For $|k_r a| \ll 1$ and $|\omega\Delta\tau| \ll 1$,

$$\frac{4}{\Delta\tau^2}\sin^2\left(\frac{\omega\Delta\tau}{2}\right) = \omega^2 - \frac{\Delta\tau^2\omega^4}{12} + \mathcal{O}(\Delta\tau^4\omega^6), \tag{9.6}$$

$$\frac{4}{a^2}\sin^2\left(\frac{k_r a}{2}\right) = k_r^2 - \frac{a^2k_r^4}{12} + \mathcal{O}(a^4k_r^6). \tag{9.7}$$

Hence

$$\omega^2 = \Omega_0^2 + c^2|\mathbf{k}|^2 + \frac{\Delta\tau^2\omega^4}{12} - \frac{c^2a^2}{12}\sum_r k_r^4 + \cdots. \tag{9.8}$$

The leading term is relativistic in form; the displayed corrections quantify temporal discretization and lattice anisotropy.

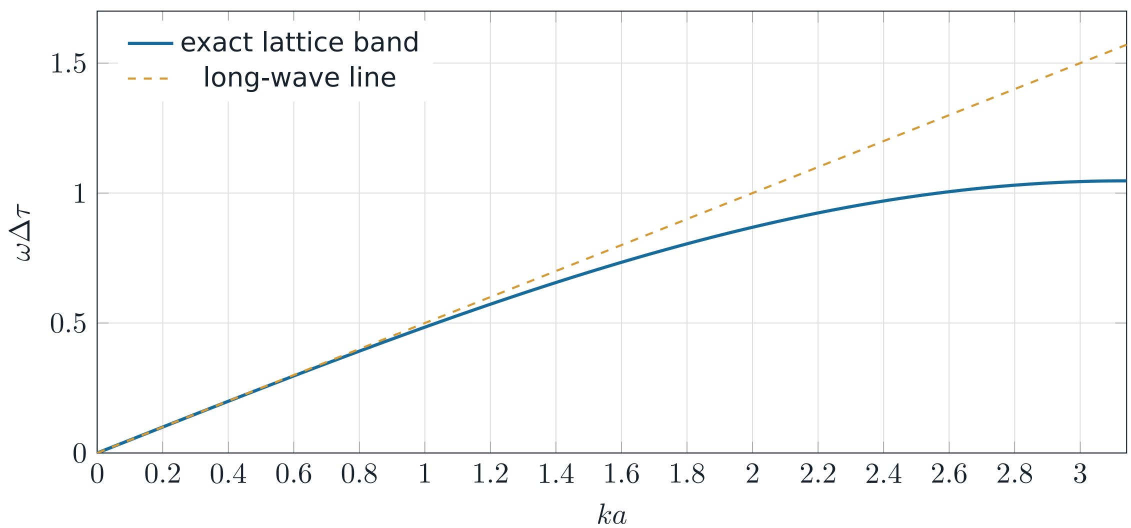

Figure 9.1: A massless one-dimensional example with $c\Delta\tau/a = 0.5$. The exact band agrees with the continuum line near $k = 0$ and bends at short wavelength.

10

Stability, speed, and the mass gap

Define

$$A(\mathbf{k}) = \Omega_0^2 + \frac{4c^2}{a^2} \sum_{r=1}^{d} \sin^2\left(\frac{k_r a}{2}\right). \tag{10.1}$$

Real ω requires the argument of the inverse sine to lie in $[0, 1]$:

$$0 \leq \frac{\Delta\tau^2}{4} A(\mathbf{k}) \leq 1. \tag{10.2}$$

The maximum occurs at a Brillouin-zone corner, where every sine squared is one. Therefore all linear modes are stable precisely when

$$\boxed{\Delta\tau^2 \left(\Omega_0^2 + \frac{4dc^2}{a^2}\right) \leq 4.} \tag{10.3}$$

PROOF PATH

Each normal coordinate obeys $Q^{n+1} - 2Q^n + Q^{n-1} + \Delta\tau^2 A Q^n = 0$. Its characteristic roots are

$$z_\pm = 1 - \frac{\Delta\tau^2 A}{2} \pm \mathrm{i}\sqrt{\Delta\tau^2 A - \frac{\Delta\tau^4 A^2}{4}}.$$

They lie on the unit circle when $0 \leq \Delta\tau^2 A \leq 4$. Beyond that interval one root has magnitude greater than one, producing exponential growth.

10.1 Group velocity

Solving Equation (9.5),

$$\omega(\mathbf{k}) = \frac{2}{\Delta\tau} \arcsin\left(\frac{\Delta\tau}{2}\sqrt{A(\mathbf{k})}\right). \tag{10.4}$$

Differentiation gives

$$v_{g,r} = \frac{\partial\omega}{\partial k_r} = \frac{(c^2/a)\sin(k_r a)}{sqrt A(\mathbf{k})\sqrt{1 - \Delta\tau^2 A(\mathbf{k})/4}}. \tag{10.5}$$

In the simultaneous long-wave and small-step limit,

$$v_{g,r} \longrightarrow \frac{c^2 k_r}{\sqrt{\Omega_0^2 + c^2|\mathbf{k}|^2}}. \tag{10.6}$$

For $\Omega_0 = 0$, the magnitude approaches c as $\mathbf{k} \to 0$.

10.2 Gap and effective mass

At $\mathbf{k} = 0$,

$$\frac{4}{\Delta\tau^2} \sin^2\left(\frac{\omega_0 \Delta\tau}{2}\right) = \Omega_0^2. \tag{10.7}$$

For a small clock step, $\omega_0 \approx \Omega_0$. After an independently established quantum action scale $\hbar$ and physical causal speed c_{phys} have been matched, a relativistic effective mass may be assigned by

$$m_{\text{eff}} c_{\text{phys}}^2 = \hbar\omega_0, \qquad m_{\text{eff}} = \frac{\hbar\omega_0}{c_{\text{phys}}^2}. \tag{10.8}$$

The gap is an internal spectral result. The conversion to kilograms or electronvolts is a physical dictionary.

WORK IT OUT

If a matched mode has $\hbar\omega_0 = 1\,\text{eV}$, then

$$m = \frac{1\,\text{eV}}{c^2} = \frac{1.602176634 \times 10^{-19}\ \text{J}}{(2.99792458 \times 10^8\ \text{m/s})^2} \approx 1.78266 \times 10^{-36}\ \text{kg}.$$

This is a unit conversion, not a new mass prediction.

11

Nonlinearity: clocks that notice amplitude

Take a uniform mode with

$$V(q) = \frac{\mu\Omega_0^2}{2}q^2 + \frac{\lambda}{4}q^4. \tag{11.1}$$

Its continuum-time equation is the Duffing oscillator

$$\ddot{q} + \Omega_0^2 q + \frac{\lambda}{\mu}q^3 = 0. \tag{11.2}$$

11.1 A perturbative frequency shift

Assume $q(t) \approx A\cos(\Omega t)$. The identity

$$\cos^3 x = \frac{3}{4}\cos x + \frac{1}{4}\cos 3x \tag{11.3}$$

shows that the cubic force contains a fundamental term and a third harmonic. Keeping the fundamental balance gives

$$-\Omega^2 A + \Omega_0^2 A + \frac{3\lambda A^3}{4\mu} \approx 0, \tag{11.4}$$

so

$$\Omega^2 \approx \Omega_0^2 + \frac{3\lambda A^2}{4\mu}. \tag{11.5}$$

For $|\lambda|A^2 \ll \mu\Omega_0^2$, expand the square root:

$$\boxed{\Omega(A) \approx \Omega_0\left(1 + \frac{3\lambda A^2}{8\mu\Omega_0^2}\right).} \tag{11.6}$$

Positive λ hardens the oscillator; negative λ softens it within the stable amplitude range.

FIRST LOOK

A small swing and a large swing need not keep exactly the same rhythm when the restoring force is nonlinear. That makes an oscillator a load-sensitive clock. End Theory's broader clock programme asks whether one local capacity mechanism can make many different clocks acquire the same low-energy dilation law.

11.2 The search for localized modes

On a graph, use the stationary ansatz

$$q_i(t) = \phi_i\cos(\Omega t) + \text{higher harmonics}. \tag{11.7}$$

Harmonic balance yields a nonlinear algebraic problem of the schematic form

$$\left[\Omega_0^2 I + \frac{\kappa}{\mu a^2}\mathsf{L} - \Omega^2 I\right]\phi + \frac{3\lambda}{4\mu}\phi^{\circ 3} = 0, \tag{11.8}$$

where $\phi^{\circ 3}$ means componentwise cubing. A continuation algorithm can begin from an anti-continuum limit, increase coupling gradually, and track the solution. Stability follows from the eigenvalues of the linearized Floquet map.

RESEARCH GATE

Search Equation (11.8) without including any known particle mass in the objective. Report dimensionless frequencies, participation ratio

$$P = \frac{(\sum_i |\phi_i|^2)^2}{\sum_i |\phi_i|^4},$$

Floquet multipliers, and persistence under graph perturbations. A small P indicates localization.

12 Phase on nodes, connection on links

Replace the real coordinate by a complex node field

$$\psi_i = \rho_i \mathrm{e}^{\mathrm{i}\theta_i} \tag{12.1}$$

and assign each oriented link a compact transporter

$$U_{ij} = \mathrm{e}^{\mathrm{i}qA_{ij}}, \qquad U_{ji} = U_{ij}^{-1}. \tag{12.2}$$

The covariant link difference is

$$D_{ij}\psi = U_{ij}\psi_j - \psi_i. \tag{12.3}$$

12.1 Exact finite-spacing invariance

Under a local phase change α_i,

$$\psi_i \mapsto \psi_i' = \mathrm{e}^{\mathrm{i}q\alpha_i}\psi_i, \qquad U_{ij} \mapsto U_{ij}' = \mathrm{e}^{\mathrm{i}q\alpha_i} U_{ij} \mathrm{e}^{-\mathrm{i}q\alpha_j}. \tag{12.4}$$

Then

$$D_{ij}'\psi' = U_{ij}'\psi_j' - \psi_i' \tag{12.5}$$
$$= \mathrm{e}^{\mathrm{i}q\alpha_i} U_{ij} \mathrm{e}^{-\mathrm{i}q\alpha_j} \mathrm{e}^{\mathrm{i}q\alpha_j}\psi_j - \mathrm{e}^{\mathrm{i}q\alpha_i}\psi_i \tag{12.6}$$
$$= \mathrm{e}^{\mathrm{i}q\alpha_i} D_{ij}\psi. \tag{12.7}$$

Therefore

$$|D_{ij}'\psi'|^2 = |D_{ij}\psi|^2. \tag{12.8}$$

This invariance is exact at finite spacing.

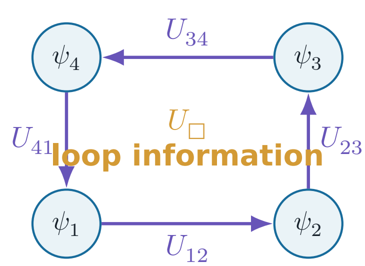

Figure 12.1: A plaquette. Node phases cancel around the closed loop, leaving gauge-invariant holonomy.

12.2 Plaquette curvature

For an oriented plaquette,

$$U_\square = U_{12}U_{23}U_{34}U_{41}. \tag{12.9}$$

All local phase factors cancel under Equation (12.4). A standard compact Abelian lattice action is

$$S_g = -\frac{\beta}{a^4} \sum_{n,\square} \Delta\tau \left(1 - \operatorname{Re} U_\square^n\right). \tag{12.10}$$

If $U_\square = \exp(\mathrm{i} q a^2 F_{\mu\nu} + \mathcal{O}(a^3))$, then

$$1 - \operatorname{Re} U_\square = \frac{1}{2} q^2 a^4 F_{\mu\nu} F^{\mu\nu} + \mathcal{O}(a^6). \tag{12.11}$$

This supplies the continuum gauge-field form after coefficient matching, following the lattice-gauge construction developed by Wilson and successors [33, 34].

12.3 Diagram language for interactions

Feynman diagrams summarize terms in a perturbative expansion; they are not pictures of tiny objects choosing routes. Once a coarse action supplies a vertex $g\phi\bar{\psi}\psi$, its lowest-order bookkeeping diagram is

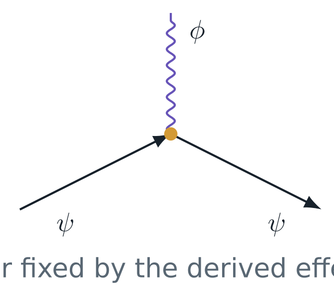

Figure 12.2: Interaction bookkeeping. End Theory reaches this diagram only after a node-pattern calculation supplies the external states and vertex coefficient.

RESEARCH GATE

Extend the link variables to a declared non-Abelian group, construct anomaly-free chiral matter, and calculate the low-energy representation content. The Nielsen–Ninomiya obstruction [39] makes this a precise mathematical design problem.

PART III

Bridges to observed physics

13

From a graph to a continuum field

A continuum limit is a controlled comparison of observables at scales much larger than the link spacing. It is not obtained by replacing a node index with the letter x. The benchmark makes the scaling explicit.

13.1 Field normalization

On a regular d-dimensional phase with cell volume a^d, define

$$q_i(t) = a^{d/2}\phi(\mathbf{x}_i, t). \tag{13.1}$$

Then

$$\sum_i q_i^2 = \sum_i a^d \phi_i^2 \longrightarrow \int \phi^2 \, \mathrm{d}^d x. \tag{13.2}$$

For a nearest-neighbour link in direction r,

$$\frac{q_{i+\hat{r}} - q_i}{a} = a^{d/2}\left(\partial_r\phi + \frac{a}{2}\partial_r^2\phi + \cdots\right). \tag{13.3}$$

Summing links therefore produces

$$\sum_{\langle ij\rangle} \frac{(q_i - q_j)^2}{a^2} \longrightarrow \int |\nabla\phi|^2 \, \mathrm{d}^d x + \mathcal{O}(a^2). \tag{13.4}$$

The continuum benchmark action is

$$S_{\text{cont}} = \int \mathrm{d}t \, \mathrm{d}^d x \left[\frac{\mu}{2}(\partial_t\phi)^2 - \frac{\kappa}{2}|\nabla\phi|^2 - V_c(\phi)\right], \tag{13.5}$$

where $V_c(\phi) = \lim_{a\to 0} a^{-d} V(a^{d/2}\phi)$ under the chosen scaling.

13.2 Matching the causal cone

Rescale to canonical time kinetic normalization with $\varphi = \sqrt{\mu}\,\phi$. Equation (13.5) becomes

$$S_{\text{cont}} = \int \mathrm{d}t \, \mathrm{d}^d x \left[\frac{1}{2}(\partial_t\varphi)^2 - \frac{c^2}{2}|\nabla\varphi|^2 - \widetilde{V}(\varphi)\right], \qquad c^2 = \frac{\kappa}{\mu}. \tag{13.6}$$

The scalar sector therefore has a low-wave-number causal speed c. A universal relativistic limit requires every light sector to share the same cone and all direction-dependent corrections to lie below observation.

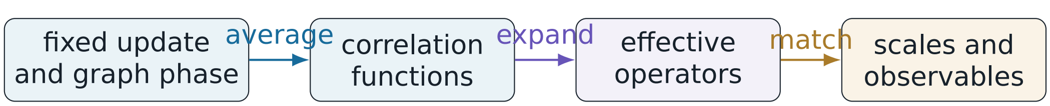

Figure 13.1: The continuum bridge. Coefficients are inferred from correlation functions and response, then matched once to physical units.

13.3 The effective-action target

At long distance, locality and symmetry organize a general action

$$S_{\text{eff}} = \int \mathrm{d}^4x\sqrt{-g}\left[\frac{M_\star^2}{2}R - \frac{1}{4}Z_{ab}F^a_{\mu\nu}F^{b\mu\nu} + \bar{\psi}\mathrm{i}e^\mu{}_a\gamma^a D_\mu\psi + \frac{1}{2}G_{AB}\partial_\mu\phi^A\partial^\mu\phi^B - U(\phi) + \sum_{n>4}\frac{c_n\mathcal{O}_n}{\Lambda^{n-4}}\right]. \tag{13.7}$$

This is a target form, using standard effective-field-theory logic [73]. End Theory becomes distinctive when the microscopic update calculates the field content, symmetries, and coefficients rather than selecting them after observation.

RESEARCH GATE

Calculate two- and four-point correlation functions on several graph refinements. Fit the same operator basis, report coefficient flow with a, and demonstrate a scale window in which irrelevant anisotropies shrink while the desired low-energy coefficients stabilize.

14

Quantum observation as a complete map

Deterministic evolution and quantum prediction address different mathematical objects. A micro-history maps one complete state to the next. An experiment reports frequencies conditioned on a preparation and a setting. A quantum completion must connect these levels explicitly.

14.1 Preparation, setting, and outcome

Let $\lambda \in \Lambda$ denote the complete micro-state relevant to one run. A preparation procedure P induces an ensemble measure

$$\mu_P(\,\mathrm{d}\lambda). \tag{14.1}$$

An apparatus setting a and response map $A(a, \lambda)$ produce an outcome. The model probability is

$$\Pr(A = x \mid a, P) = \int_\Lambda \mathbf{1}[A(a, \lambda) = x]\, \mu_P(\,\mathrm{d}\lambda). \tag{14.2}$$

The Born-rule target for a quantum state ρ_P and measurement operators $E_x^{(a)}$ is

$$\Pr(A = x \mid a, P) = \mathrm{Tr}\Big(\rho_P E_x^{(a)}\Big)\,. \tag{14.3}$$

Recovering Equation (14.3) is a calculation of ensemble frequencies; calling the micro-update chaotic does not perform the integral.

FIRST LOOK

A coin can follow ordinary mechanics and still look random when you do not know its exact launch. Quantum theory asks for a much more specific pattern of probabilities, including interference and entanglement. The task is not to say “hidden details exist.” The task is to calculate the exact observed frequency from the hidden details.

14.2 Bell–CHSH as a design constraint

For two separated wings with settings a, a' and b, b', outcomes $A, B \in \{-1, +1\}$ define correlations

$$E(a, b) = \int A(a, \lambda)B(b, \lambda)\rho(\lambda)\,\mathrm{d}\lambda. \tag{14.4}$$

Local response and measurement independence imply the CHSH bound

$$S = |E(a, b) + E(a, b') + E(a', b) - E(a', b')| \le 2. \tag{14.5}$$

Quantum mechanics reaches $2\sqrt{2}$, and loophole-controlled experiments violate the local bound [79, 86, 84]. A deterministic End Theory completion must identify, in equations, the probability structure that changes one of the assumptions used to derive Equation (14.5).

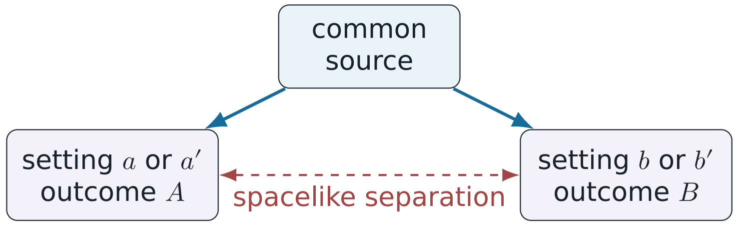

Figure 14.1: Bell-test structure. The preparation distribution, setting dependence, local response, and outcome map must all be declared.

14.3 Operational no-signalling

Whatever completion is chosen, the observable marginal on one wing must not depend on the remote freely varied setting:

$$\sum_y \Pr(x, y \mid a, b, P) = \sum_y \Pr(x, y \mid a, b', P). \tag{14.6}$$

This is an empirical constraint on the outcome distribution. It can coexist with correlations that violate Equation (14.5).

14.4 Localization as a measurable process

A capacity threshold may participate in amplification if a declared functional $T[X; \mathcal{R}]$ over detector region $\mathcal{R}$ reaches a fixed value $T_\star$. A complete model then specifies

$$T < T_\star : \text{distributed response}, \qquad T \geq T_\star : \text{stable outcome channel}, \tag{14.7}$$

and calculates the frequency of channels across the preparation ensemble. Conservation is checked by including the apparatus and environment in the balance law.

RESEARCH GATE

Choose one two-path interference experiment. Define P, λ, the phase-control setting, the detector amplification map, and the ensemble measure. Recover the fringe law and vary a which-path coupling without changing the model parameters.

15

Geometry, gravity, and torsion

Gravity enters only after clocks, rods, propagation, and coarse geometry exist. The bridge has three levels: reconstruct a metric, derive its universal coupling to matter, and calculate the effective action governing its response.

15.1 Metric from operational intervals

Suppose stable signal modes define local travel times and clock patterns define durations. At long wavelength, fit the eikonal relation

$$g^{\mu\nu}(x)k_\mu k_\nu = 0 \tag{15.1}$$

for several independent massless sectors. A common $g^{\mu\nu}$ defines the causal geometry. Massive pattern trajectories should then approach

$$\frac{\mathrm{d}^2x^\mu}{\mathrm{d}s^2} + \Gamma^\mu_{\nu\rho}\frac{\mathrm{d}x^\nu}{\mathrm{d}s}\frac{\mathrm{d}x^\rho}{\mathrm{d}s} = 0 \tag{15.2}$$

with the same connection, up to controlled spin or finite-size effects.

15.2 Torsion as loop nonclosure

With tetrad one-forms e^a and spin connection $\omega^a{}_b$, torsion is

$$T^a = \mathrm{d}e^a + \omega^a{}_b \wedge e^b. \tag{15.3}$$

For two small displacement vectors u and v, the leading failure of a transported parallelogram to close is

$$\Delta x^\mu = T^\mu_{\nu\rho}u^\nu v^\rho + \mathcal{O}(|u|^2|v|, |u||v|^2). \tag{15.4}$$

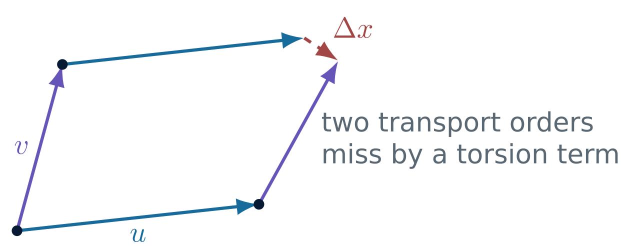

Figure 15.1: A geometric interpretation of torsion. A node model must derive the transport rule before assigning the mismatch.

The phrase "progression imbalance" can be given a disciplined meaning by calculating a coarse transport nonclosure and identifying it with Equation (15.3). In Riemann–Cartan gravity, spin can source torsion [94]; the effective coefficients must be obtained from the coarse node response.

15.3 Newtonian and Einstein targets

In the weak static limit, write

$$g_{00} \approx -\left(1 + \frac{2\Phi_N}{c^2}\right). \tag{15.5}$$

The required long-distance equation is

$$\nabla^2 \Phi_N = 4\pi G \rho. \tag{15.6}$$

At the covariant level, the Einstein–Hilbert term is

$$S_{\mathrm{EH}} = \frac{c^3}{16\pi G} \int R\sqrt{-g}\, \mathrm{d}^4 x, \tag{15.7}$$

with additional torsion terms if the independent connection persists. The bridge calculation has a clear output: derive Equation (15.7), determine G from microscopic parameters, recover Equation (15.6), and test universal free fall.

WORK IT OUT

For a spherical mass M, solve $\nabla^2 \Phi = 0$ outside the source. Spherical symmetry gives

$$\frac{1}{r^2}\frac{\mathrm{d}}{\mathrm{d}r}\left(r^2 \frac{\mathrm{d}\Phi}{\mathrm{d}r}\right) = 0.$$

Integrate twice: $r^2 \Phi' = C_1$, so $\Phi = -C_1/r + C_2$. Matching to Equation (15.6) fixes $C_1 = GM$ and a zero at infinity fixes $C_2 = 0$.

16

Residual capacity and the EQEF sector

EQEF is used here in one controlled sense: it is the coarse description of expressed and deferred local transition capacity. At the discrete level the primary quantity is the residual ledger $r_i^n = 1 - C_i^n$.

16.1 A causal balance law

Let $J_{ij}^n = -J_{ji}^n$ be residual-capacity transport along a link and s_i^n a local conversion term. A candidate balance equation is

$$r_i^{n+1} - r_i^n + \sum_{j\sim i} J_{ij}^n = s_i^n. \tag{16.1}$$

Summing over a finite region $\mathcal{R}$ cancels internal link currents:

$$\sum_{i\in\mathcal{R}} (r_i^{n+1} - r_i^n) + \sum_{\substack{i\in\mathcal{R}\\ j\notin\mathcal{R}}} J_{ij}^n = \sum_{i\in\mathcal{R}} s_i^n. \tag{16.2}$$

This is the desired causal structure: change in a region equals boundary flux plus local conversion.

16.2 Coarse field

Choose a normalized kernel $K_R(x,i)$ and background $\bar{r}$. Define

$$\chi_R(x) = Z_R \sum_i K_R(x,i)(r_i - \bar{r}). \tag{16.3}$$

A conservative scalar effective action may take the form

$$S_\chi = \int \sqrt{-g}\, \mathrm{d}^4x \left[-\frac{Z_\chi}{2} g^{\mu\nu} \partial_\mu \chi \partial_\nu \chi - U(\chi) - \frac{\xi}{2}\chi^2 R \right]. \tag{16.4}$$

The microscopic calculation must determine the sign of Z_χ, the potential, the coupling ξ, and the source map. Positivity $Z_\chi > 0$ supplies the ordinary second-order kinetic sector.

16.3 Homogeneous cosmology target

For a spatially flat Friedmann–Lemaître–Robertson–Walker metric and homogeneous $\chi(t)$, minimal coupling gives

$$\rho_\chi = \frac{Z_\chi}{2}\dot{\chi}^2 + U(\chi), \tag{16.5}$$

$$p_\chi = \frac{Z_\chi}{2}\dot{\chi}^2 - U(\chi), \tag{16.6}$$

$$\ddot{\chi} + 3H\dot{\chi} + Z_\chi^{-1} U'(\chi) = 0, \tag{16.7}$$

with Friedmann equation

$$H^2 = \frac{8\pi G}{3} \left(\rho_{\text{known}} + \rho_\chi\right) \tag{16.8}$$

after the gravitational bridge has been established. Perturbations $\delta\chi$ then determine structure and microwave-background consequences. The model parameters are frozen before those spectra are opened.

FIRST LOOK

Residual capacity is like unused room in a local schedule. A region can store it, pass it to neighbours, or convert it through a declared rule. A cosmic field is justified only when many local ledgers average into one smooth variable with its own measured response.

17

Constants, units, and honest dependencies

Constants enter a theory in different ways. Some define units. Some are measured independent scales. Some are algebraic combinations. A small number may eventually be genuine outputs of a microscopic spectrum. Clear classification prevents a familiar identity from being counted as a new prediction.

17.1 The four-level ladder

Level	Operation	Example
Definition	Fixes a unit or convention	$c = 299792458\,\mathrm{m/s}$ in SI
Identity	Recombines established quantities	$E = mc^2$, $\hbar = h/(2\pi)$
Matching	Equates a model coefficient to a measured scale	$c_{\text{model}} a/\Delta\tau = c_{\text{SI}}$
Prediction	Calculates a held-out dimensionless or dimensional observable after matching	A new mass ratio from two independently identified pattern gaps

Table 17.1: A constant's numerical agreement has meaning only after its operation is classified.

17.2 Planck combinations, fully worked

Using $\hbar$, c, G, and k_B, the standard Planck combinations are

$$\ell_P = \sqrt{\frac{\hbar G}{c^3}} \approx 1.616255e-35\,\mathrm{m}, \tag{17.1}$$

$$t_P = \sqrt{\frac{\hbar G}{c^5}} \approx 5.391247e-44\,\mathrm{s}, \tag{17.2}$$

$$m_P = \sqrt{\frac{\hbar c}{G}} \approx 2.176434e-8\,\mathrm{kg}, \tag{17.3}$$

$$E_P = m_P c^2 \approx 1.95608e9\,\mathrm{J}, \tag{17.4}$$

$$T_P = \frac{E_P}{k_B} \approx 1.41678e32\,\mathrm{K}. \tag{17.5}$$

These are dependency calculations: G, $\hbar$, c, and k_B are inputs.

The area of a sphere of radius ℓ_P is

$$A_{P,\text{sphere}} = 4\pi\ell_P^2 \approx 3.283e-69\,\mathrm{m}^2. \tag{17.6}$$

Planck power is

$$P_P = \frac{E_P}{t_P} = \frac{c^5}{G} \approx 3.628e52\,\mathrm{W}. \tag{17.7}$$

17.3 Blackbody radiation

Planck's spectral energy density per angular frequency is

$$u_\omega(T) = \frac{\hbar\omega^3}{\pi^2 c^3}\frac{1}{\exp(\hbar\omega/k_B T) - 1}. \tag{17.8}$$

Integrate with $x = \hbar\omega/(k_B T)$:

$$\begin{aligned} u(T) &= \int_0^\infty u_\omega \, \mathrm{d}\omega \qquad (17.9)\\ &= \frac{(k_B T)^4}{\pi^2\hbar^3 c^3}\int_0^\infty \frac{x^3}{\mathrm{e}^x - 1}\,\mathrm{d}x \qquad (17.10)\\ &= \frac{\pi^2 k_B^4}{15\hbar^3 c^3}T^4, \qquad (17.11)\end{aligned}$$

because the integral is $\pi^4/15$. Isotropic radiation carries outward flux $F = cu/4$, so

$$F = \sigma T^4, \qquad \boxed{\sigma = \frac{\pi^2 k_B^4}{60\hbar^3 c^2}} \approx 5.670374419e - 8\,\mathrm{W.m^{-2}.K^{-4}}. \tag{17.12}$$

This derives the Stefan–Boltzmann constant from the quantum radiation law and SI defining constants; it is not a separate End Theory output.

17.4 Electromagnetic coupling

In SI,

$$\alpha = \frac{e^2}{4\pi\varepsilon_0\hbar c}. \tag{17.13}$$

Today e, h, and c are exact SI defining constants, while ε_0 is experimentally related through the fine-structure constant. A lattice theory predicts α only if its bare charge content and renormalization flow determine the low-energy dimensionless coupling without using the target value.

17.5 Strong coupling: a corrected one-loop example

At one loop,

$$\alpha_s(Q) = \frac{4\pi}{\beta_0 \ln(Q^2/\Lambda^2)}, \qquad \beta_0 = 11 - \frac{2n_f}{3}. \tag{17.14}$$

For $n_f = 5$, $Q = 91.1876\,\mathrm{GeV}$, and $\Lambda = 0.213\,\mathrm{GeV}$,

$$\beta_0 = \frac{23}{3}, \qquad \ln(Q^2/\Lambda^2) \approx 12.12, \tag{17.15}$$

so the one-loop value is approximately 0.135, not 0.118. Higher-loop running and scheme-dependent threshold matching change the relation between Λ_{QCD} and $\alpha_s(M_Z)$. Reversing Equation (17.14) at one loop to match 0.118 gives an illustrative $\Lambda \approx 0.088\,\mathrm{GeV}$. Precision work uses the declared loop order and scheme [117].

17.6 A natural-unit cross-section example

Suppose a contact estimate is

$$\sigma \sim \frac{g^2}{4\pi m^2}. \tag{17.16}$$

With $g = 10^{-2}$ and $m = 100\,\text{GeV}$,

$$\sigma \approx 7.96 \times 10^{-10}\ \text{GeV}^{-2}. \tag{17.17}$$

Using 1 $\text{GeV}^{-2} = 0.389379 \times 10^{-27}\ \text{cm}^2$,

$$\sigma \approx 3.10 \times 10^{-37}\ \text{cm}^2. \tag{17.18}$$

The conversion line is essential; a result written directly in square centimetres without it cannot be audited.

17.7 A solar-mass black hole

For $M = M_\odot \approx 1.98847e30\,\text{kg}$,

$$r_s = \frac{2GM}{c^2} \approx 2.953\,\text{km}. \tag{17.19}$$

The Bekenstein–Hawking entropy is

$$S_{\text{BH}} = \frac{k_B A}{4\ell_P^2} = \frac{k_B \pi r_s^2}{\ell_P^2} \approx 1.45 \times 10^{54}\ \text{J/K}, \tag{17.20}$$

or $S_{\text{BH}}/k_B \approx 1.05 \times 10^{77}$ dimensionless information units. The units distinguish those two quoted magnitudes.

RESEARCH GATE

For every proposed constant, print an input ledger: formula, dimensions, numerical inputs, covariance, scale and scheme, calibration/hold-out assignment, and code checksum. The next strong End Theory result should be a dimensionless ratio or scaling exponent calculated before its comparison value is opened.

18

Complex adaptive systems as a later layer

The relational language can also describe biological or artificial networks, but this layer begins after the physical theory has supplied time, energy, matter, and measurement. It is therefore kept separate from the foundational action.

18.1 Memory as persistent state

Let $z_i(t) = r_i(t)\mathrm{e}^{\mathrm{i}\theta_i(t)}$ represent coarse activity in subsystem i. A memory candidate is a metastable attractor $\mathcal{A}_m$ whose return probability after a standardized perturbation is

$$R_m(\Delta) = \Pr[z(t+\Delta) \in \mathcal{A}_m \mid z(t) \in \mathcal{A}_m,\ \text{probe}]\,. \tag{18.1}$$

This turns "persistent configuration" into an experimental statistic.

18.2 Phase coordination

A standard synchronization order parameter is

$$\mathcal{R}(t)\mathrm{e}^{\mathrm{i}\Psi(t)} = \frac{1}{N}\sum_{j=1}^{N} \mathrm{e}^{\mathrm{i}\theta_j(t)}, \qquad 0 \le \mathcal{R} \le 1. \tag{18.2}$$

Large $\mathcal{R}$ indicates phase alignment, but alignment alone is not awareness. A testable integrative index may combine coordination, causal influence, and adaptive prediction:

$$\mathcal{I}_T = \frac{1}{T}\int_{t_0}^{t_0+T} \mathcal{R}(t)\,\mathcal{C}(t)\,\mathcal{P}(t)\,\mathrm{d}t, \tag{18.3}$$

where each factor is normalized and independently operationalized. Equation (18.3) is a phenomenological research definition, not a fundamental law.

FIRST LOOK

Many musicians can play the same beat, yet a good orchestra also listens, predicts, corrects mistakes, and remembers the score. Synchrony measures only the shared beat. A serious theory of awareness must measure the additional causal and adaptive structure.

18.3 A clean research boundary

Claims about attention, temporal perception, memory, and self-maintaining feedback can be studied through perturbation recovery, information flow, phase coordination, and behavioural report. They enter End Theory as applications of a mature relational dynamics, not as evidence for the fundamental node model.

PART IV

Wave observation and verification manual

19

Wave observation theory

A wave equation becomes experimental only after a source, propagation law, sensor response, sampling rule, and likelihood are connected. This chapter defines that chain in a form that can be used for lattice simulations, laboratory waves, gravitational signals, or collider distributions.

19.1 The observation chain

Let $s(t, \mathbf{x}; \vartheta)$ be a source with parameters ϑ. A Green function G propagates it to a field

$$\phi(t, \mathbf{x}) = \int G(t - t', \mathbf{x}, \mathbf{x}'; p) s(t', \mathbf{x}'; \vartheta) \, \mathrm{d}t' \, \mathrm{d}^d x'. \tag{19.1}$$

A detector with response kernel R_a produces channel a:

$$y_a(t) = \int R_a(t - t', \mathbf{x}') \phi(t', \mathbf{x}') \, \mathrm{d}t' \, \mathrm{d}^d x' + n_a(t), \tag{19.2}$$

where n_a is noise. Sampling at times t_m gives data vector $\mathbf{y}$.

Figure 19.1: A complete observation map. Each block has parameters, calibration data, uncertainty, and a validation test.

For Gaussian noise with covariance C and model mean $\mathbf{m}(p, \vartheta)$,

$$-2 \ln \mathcal{L} = (\mathbf{y} - \mathbf{m})^{\mathsf{T}} C^{-1} (\mathbf{y} - \mathbf{m}) + \ln \det C + \text{constant}. \tag{19.3}$$

Non-Gaussian counting or threshold data use the corresponding likelihood rather than forcing a least-squares form.

19.2 Reading dispersion from phase

For two sensors separated by L along propagation, the cross spectrum is

$$C_{12}(\omega) = \tilde{y}_1^*(\omega) \tilde{y}_2(\omega). \tag{19.4}$$

Its phase $\Delta\varphi(\omega) = \arg C_{12}$ estimates

$$k(\omega) = \frac{\text{unwrap}\, \Delta\varphi(\omega)}{L}, \tag{19.5}$$

after accounting for the response-phase difference of the sensors. Comparing $k(\omega)$ with Equation (9.5) tests the lattice band without fitting a particle identity.

WORK IT OUT

Two probes are $L = 3\,\text{m}$ apart. At $f = 20\,\text{Hz}$ the calibrated cross-phase is 1.50 rad. Then $k = 1.50/3 = 0.50\,\text{rad.m}^{-1}$ and $\omega = 2\pi f \approx 125.66\,\text{rad.s}^{-1}$. The phase velocity is

$$v_p = \omega/k \approx 251.3\,\text{m/s}.$$

Repeat across frequency; a single point cannot determine dispersion.

19.3 Sampling and aliases

With sampling interval Δt_s, the Nyquist frequency is

$$f_N = \frac{1}{2\Delta t_s}. \tag{19.6}$$

A frequency $f > f_N$ aliases to a lower observed frequency. Spatial sampling on a regular graph has the parallel limit $|k_r| \le \pi/a$. The Brillouin-zone edge in the exact dispersion relation is therefore not a decorative mathematical boundary; it is the shortest distinct wavelength represented by the lattice.

19.4 A wave-result ledger

Every reported wave result records:

1. source waveform and nuisance parameters;
2. propagation equation and boundary conditions;
3. sensor transfer function and calibration covariance;
4. sample rate, window, filtering, and missing-data policy;
5. estimator and uncertainty;
6. baseline model;
7. held-out frequency or geometry range;
8. pass/fail rule fixed before opening the hold-out.

20

The reproducible lattice laboratory

The first executable project verifies the benchmark before attaching it to known particles. Use periodic chains, square/cubic lattices, and approximately isotropic irregular graphs. The program should reproduce the exact spectrum, stability boundary, gauge invariants, and refinement behaviour.

20.1 Minimal scalar update

```
inputs: graph W, mu, kappa, a, dt, Omega0, nonlinear dW(q)
state:  q_prev, q_now

repeat for n = 0 ... N-1:
    lap = (degree(W) - W) @ q_now
    force = (kappa/a^2) * lap + mu*Omega0^2*q_now + dW(q_now)
    q_next = 2*q_now - q_prev - (dt^2/mu) * force
    record observables(q_prev, q_now, q_next)
    q_prev, q_now = q_now, q_next
```

The implementation test for one eigenmode u_r with Laplacian eigenvalue λ_r is

$$\omega_r^{\mathrm{exact}} = \frac{2}{\Delta\tau} \arcsin\left[\frac{\Delta\tau}{2}\sqrt{\Omega_0^2 + \frac{\kappa\lambda_r}{\mu a^2}}\right]. \tag{20.1}$$

20.2 Initial data for a pure mode

Choose amplitude A and phase φ:

$$q^0 = Au_r \cos\varphi, \tag{20.2}$$
$$q^1 = Au_r \cos(\varphi - \omega_r\Delta\tau). \tag{20.3}$$

Project the trajectory back onto the mode,

$$Q_r^n = (u_r)^{\mathsf{T}} q^n, \tag{20.4}$$

and fit its phase. The relative frequency residual is

$$\epsilon_\omega = \frac{\widehat{\omega}_r - \omega_r^{\mathrm{exact}}}{\omega_r^{\mathrm{exact}}}. \tag{20.5}$$

20.3 Gauge-invariance unit test

Generate random node phases α_i. Transform ψ and U by Equation (12.4). Compute

$$\epsilon_D = \frac{\left|\sum_{\langle ij\rangle} |D'_{ij}\psi'|^2 - \sum_{\langle ij\rangle} |D_{ij}\psi|^2\right|}{\max\left(1, \sum_{\langle ij\rangle} |D_{ij}\psi|^2\right)}. \tag{20.6}$$

Double-precision code should place ϵ_D near its accumulated floating-point tolerance.

20.4 Refinement study

Let an observable have leading error $O(a^p)$. For spacings a, $a/2$, and $a/4$, the differences satisfy

$$\frac{O(a) - O(a/2)}{O(a/2) - O(a/4)} \longrightarrow 2^p. \tag{20.7}$$

Estimate

$$\hat{p} = \log_2 \left| \frac{O(a) - O(a/2)}{O(a/2) - O(a/4)} \right|. \tag{20.8}$$

This separates a continuum trend from a single attractive plot.

Test	**Procedure**	**Pass record**
Normal modes	Initialize each Laplacian eigenvector	Frequency residual vs. precision and duration
Stability edge	Sweep $\Delta\tau$ across Equation (10.3)	Growth begins at the analytic boundary within scan resolution
Invariant	Track Equation (8.12)	Bounded roundoff-scale drift in the linear stable sector
Gauge transform	Random local phase rotations	ϵ_D and plaquette differences at floating-point tolerance
Refinement	Repeat fixed physical initial data	Estimated order $\hat{p}$ and extrapolated observable
Irregular graphs	Compare isotropy estimators	Directional residual distribution and spectral dimension

Table 20.1: Core verification suite. Thresholds are recorded numerically in the project's parameter card.

DRY NOTE FROM THE FLIGHT DECK

"The plot looked stable" is not a unit test. It is a plot wearing a lab coat.

21

CERN-facing interaction templates

The microscopic framework currently supplies exact benchmark structure rather than a unique collider mass. CERN analysis can still be prepared through parameterized templates, with every coefficient labeled as matching input until a node-pattern calculation fixes it.

21.1 Neutral scalar template

For a neutral scalar pattern s, a low-energy interaction basis may include

$$\mathcal{L}_s = \frac{1}{2}(\partial s)^2 - \frac{1}{2}m_s^2 s^2 - \frac{\lambda_{sH}}{2}s^2 H^\dagger H - \sum_f y_f^{(s)} s\bar{f}f - \frac{c_g}{4\Lambda}sG^a_{\mu\nu}G^{a\mu\nu} - \frac{c_\gamma}{4\Lambda}sF_{\mu\nu}F^{\mu\nu}. \tag{21.1}$$

A microscopic calculation must identify the pattern, normalize its state, and compute m_s, λ_{sH}, $y_f^{(s)}$, c_g, and c_γ.

21.2 Contact correction template

High-energy deviations can be organized by dimension-six operators such as

$$\mathcal{L}_{\text{contact}} = \sum_i \frac{C_i}{\Lambda^2}\mathcal{O}_i. \tag{21.2}$$

The event-level validity region $\hat{s} < \Lambda^2_{\text{valid}}$ is applied before the fit. Limits then constrain coefficient combinations; they become End Theory tests only after the micro-to-operator map is frozen.

21.3 Binned likelihood

For observed counts n_b and expected counts

$$\nu_b(\theta,\eta) = s_b(\theta,\eta) + b_b(\eta), \tag{21.3}$$

use

$$\mathcal{L}(\theta,\eta) = \prod_b \frac{\nu_b^{n_b}\mathrm{e}^{-\nu_b}}{n_b!}\prod_k \pi_k(\eta_k), \tag{21.4}$$

where η are nuisance parameters with constraint terms π_k. Correlated systematic effects are shared across bins and channels rather than added independently in quadrature when a covariance is available.

21.4 Open-data entry point

CERN's ATLAS 13 TeV educational release provides 10 fb^{-1} of 2016 proton–proton data with matched simulated samples, including four-lepton and diphoton collections [120, 121]. It is suitable for learning the analysis chain and reproducing public examples. A research-grade claim uses the collaboration's current analysis objects, calibrations, and likelihood information.

RESEARCH GATE

Build the likelihood with a background-only model and one template coefficient. Validate it on a known injected signal. Freeze event selection, binning, nuisance correlations, and the validity cut before opening the held-out distribution.

22

Evidence without retrofitting

Let the full parameter vector be split into structural parameters p_s, calibration parameters p_c, and nuisance parameters η. A clean protocol assigns data once:

$$D = D_{\text{design}} \cup D_{\text{cal}} \cup D_{\text{test}}, \qquad D_{\text{cal}} \cap D_{\text{test}} = \emptyset. \tag{22.1}$$

22.1 Freeze before comparison

The model card contains

$$\mathcal{C}_{\text{model}} = \{\text{equations, graph rule, } p_s, p_c, \text{ priors, code version, seeds, units, data IDs}\}. \tag{22.2}$$

Hash the card and code. The prediction function is then

$$\hat{\mathbf{y}}_{\text{test}} = F(\mathcal{C}_{\text{model}}, D_{\text{cal}}; X_{\text{test}}), \tag{22.3}$$

evaluated without changing $\mathcal{C}_{\text{model}}$.

22.2 Uncertainty propagation

For outputs $\mathbf{y} = f(\mathbf{x})$ and input covariance V_x, the linearized covariance is

$$V_y = J V_x J^\mathsf{T}, \qquad J_{ij} = \frac{\partial f_i}{\partial x_j}. \tag{22.4}$$

For one multiplicative quantity $Q = \prod_j x_j^{a_j}$,

$$\frac{u^2(Q)}{Q^2} = \sum_{ij} a_i a_j \frac{\text{Cov}(x_i, x_j)}{x_i x_j}. \tag{22.5}$$

Ignoring covariance can either inflate or shrink the final uncertainty.

22.3 Model comparison

Report absolute fit and improvement over a baseline. For nested models, a profile likelihood statistic is

$$q = -2 \ln \frac{\mathcal{L}(\theta_0, \hat{\hat{\eta}})}{\mathcal{L}(\hat{\theta}, \hat{\eta})}. \tag{22.6}$$

Also report parameter count, prior volume where relevant, residual structure, robustness to declared alternatives, and negative results.

WORK IT OUT

Suppose $Q = x^2/y$, with $x = 3.0 \pm 0.1$, $y = 2.0 \pm 0.2$, and zero covariance. Then $Q = 4.5$ and

$$\frac{u^2(Q)}{Q^2} = 4\left(\frac{0.1}{3.0}\right)^2 + \left(\frac{0.2}{2.0}\right)^2 = 0.01444.$$

Thus $u(Q) = 4.5\sqrt{0.01444} \approx 0.54$, so $Q = 4.50 \pm 0.54$ at one standard uncertainty.

23

The falsification ladder

The research programme advances through gates in dependency order. Passing a later-looking comparison does not repair an earlier undefined bridge.

Gate	Object	Required calculation	Decision record
1	Benchmark dynamics	Exact update, spectrum, invariant, stability, gauge test	Reproduction logs and tolerances
2	Capacity completion	Closure, locality, deterministic tie-breaks, conservation	Proof plus saturation stress tests
3	Emergent geometry	Persistence, graph construction, dimension plateau, isotropy, clocks	Scale window and failure regions
4	Pattern spectrum	Localized solutions, stability, dispersion, scattering	Blind dimensionless catalogue
5	Known fields	Gauge group, chirality, representations, anomaly cancellation	Derived low-energy operator content
6	Quantum map	Preparation ensemble, Born frequencies, Bell assumption, no-signalling	Preregistered interference and Bell simulations
7	Gravity/EQEF	Common metric, Newtonian/Einstein limit, torsion and capacity sources	Solar-system, wave, and cosmology likelihoods
8	Prediction	Frozen calibration and held-out observable	External comparison with uncertainty

23.1 Decision logic for a new idea

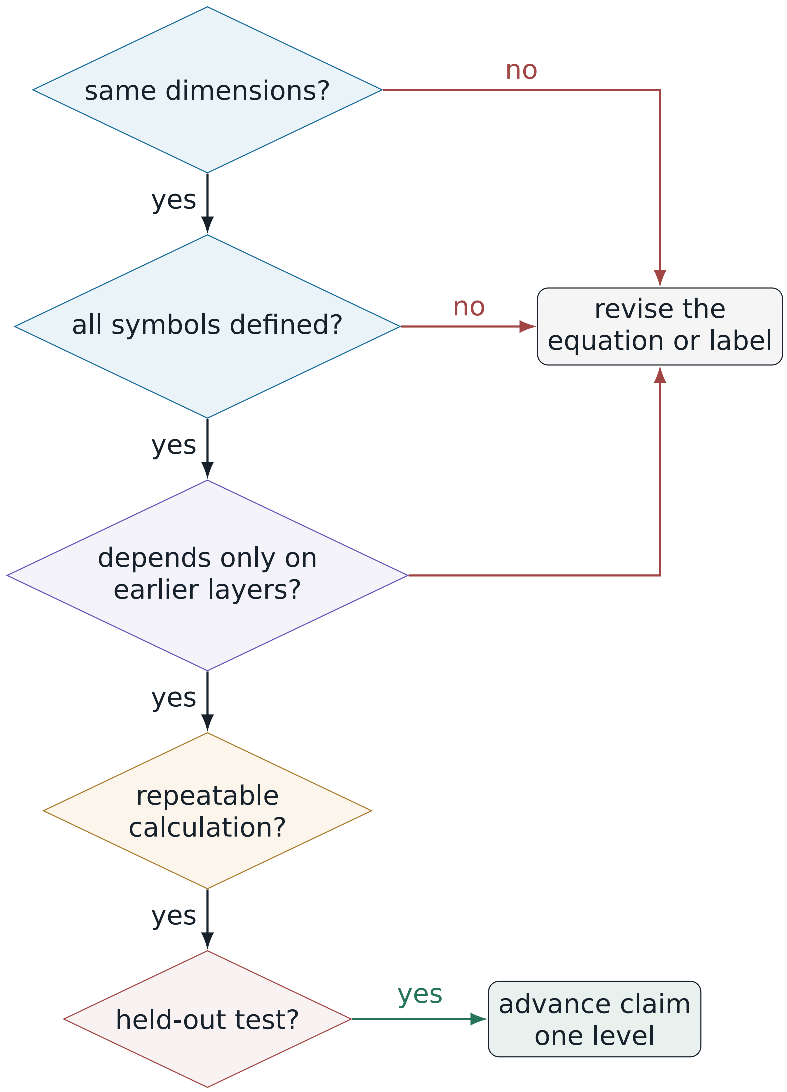

Figure 23.1: A compact author decision tool. The label changes only after the corresponding operation has been completed.

23.2 The completion criterion

End Theory becomes a quantitatively competitive physical theory when one immutable micro-model crosses the gates with fewer calibrated inputs than independent held-out results, publishes its negative regions, and remains stable under independent reproduction. Until then, the scientifically useful object is the ordered framework, exact benchmark, and explicit programme recorded in this textbook.

DRY NOTE FROM THE FLIGHT DECK

Changing the finish line after the race is excellent exercise and poor inference.

PART V

The End Theory concept atlas

How to use the atlas

The atlas is ordered by dependency. Each topic occupies a compact statement page followed by a working page. The first page tells the reader what the object means; the second records inputs, algebra, dimensions, and the calculation that advances it.

Relational proto-state

DEFINED

Compact equation

$$\mathcal{P} = (\mathcal{X}, \mathcal{R}, \mathcal{A}, U_p), \quad X_n \notin \mathcal{M}_{\text{spacetime}}$$

FIRST LOOK

Begin with possible states, direct relations, legal local changes, and an update. Physical distance and duration are later observables.

Dependency: None; this is the root definition.

F01 Working page: Relational proto-state

Derivation or construction

Choose a finite alphabet Σ and a relational hypergraph H_n. One explicit prototype is $X_n = (H_n, s_n)$ with $s_n : V(H_n) \to \Sigma$. Locality means $[U_p(X)]_i$ depends on a bounded relational neighbourhood.

Dimensions and normalization

The primitive labels are dimensionless unless the model explicitly assigns a scale. Metres and seconds enter only through derived rods and clocks.

Decisive calculation

Run the update without a coordinate embedding. If the rule requires Euclidean distance to decide which primitive elements interact, the pre-geometric claim has been replaced by a background geometry.

READER CHECK

Name every object needed to compute X_1 from X_0. Circle any object whose definition already assumes position, time, energy, or particle identity.

Ordered updates before time

DEFINED

Compact equation

$$X_{n+1} = U_p(X_n), \qquad n \in \mathbb{Z}$$

FIRST LOOK

The index orders snapshots. A clock reading is built from a stable repeating process inside the snapshots.

Dependency: F01: relational proto-state and update.

F02 Working page: Ordered updates before time

Derivation or construction

Iterate one fixed map to form the history $\Gamma(X_0) = \{X_0, U_p X_0, U_p^2 X_0, ...\}$. Causal order means effects at step $n+1$ depend only on the declared past neighbourhood.

Dimensions and normalization

n is dimensionless. A conversion $t = n\Delta t$ is a homogeneous matching rule unless Δt is generated by clock dynamics.

Decisive calculation

Verify that histories are single-valued and that changing the update schedule does not change observables unless the schedule itself is part of the state.

READER CHECK

A process repeats every 12 updates. If one period is calibrated as 0.75 s, compute the homogeneous duration per update: $0.75/12 = 0.0625$ s. Label the operation as matching.

Operational clock map

PROPOSED

Compact equation

$$N_K(n) = \frac{\mathrm{unwrap}\,\Theta_K(n)}{2\pi}, \qquad t_K = T_K N_K$$

FIRST LOOK

A clock is a robust orbit whose phase can be counted. Time is what the orbit reads, not the name of the update counter.

Dependency: F02 and a persistent recurrent subsystem.

F03 Working page: Operational clock map

Derivation or construction

Select a complex observable $Z_K = A_K e^{i\Theta_K}$. Unwrap its phase and count crossings of 2π. Linearize one period to obtain a monodromy matrix; transverse multipliers inside the unit circle indicate recovery from small disturbances.

Dimensions and normalization

N_K and Θ_K are dimensionless. T_K carries time and must be calibrated once or related to another predicted scale.

Decisive calculation

Build two clock types. In a common low-load regime, test whether their rate ratio approaches a constant and whether imposed load changes both rates by the same factor.

READER CHECK

If Θ_K advances by $\pi/8$ per update, show that one cycle takes 16 updates.

Persistence across frames

DEFINED

Compact equation

$$\inf_{g \in \mathcal{G}_R} d_R(C_R X_{n+T}, g C_R X_n) < \varepsilon_R$$

FIRST LOOK

A pattern keeps its identity when coarse features stay close after an allowed motion, phase change, or relabeling.

Dependency: F01–F03 and a declared resolution.

F04 Working page: Persistence across frames

Derivation or construction

Fix C_R, d_R, $\mathcal{G}_R$, and ε_R before searching. Define the equivalence tube $[X]_{R,\varepsilon}$ and record first-exit time τ_R. Compare τ_R with the internal cycle period.

Dimensions and normalization

d_R is dimensionless or normalized by a fixed scale. T counts updates until an operational clock is applied.

Decisive calculation

Perturb pattern candidates and measure the lifetime distribution across resolutions. Robust classes show a plateau rather than appearing only at one tuned tolerance.

READER CHECK

Explain why a translated wave packet can remain the same pattern even though its node-by-node vector has changed.

Emergent weighted graph

PROPOSED

Compact equation

$$w_{ab} = \frac{1}{T}\sum_{n=1}^{T} I_{ab}(n), \qquad G_R = (V_R, E_R, W_R)$$

FIRST LOOK

Tap one persistent pattern and measure which other patterns respond. The response network draws effective neighbourhood.

Dependency: F04 persistent classes and an intervention rule.

F05 Working page: Emergent weighted graph

Derivation or construction

Perturb class a by standardized δ, measure resolved response in b, normalize by $\|\delta\|$, and average over a fixed window. Retain a link when $w_{ab} > w_{\min}$. Keep direction until reciprocity is demonstrated.

Dimensions and normalization

I_{ab} and w_{ab} are dimensionless response ratios. Physical link length requires a separate scale and function $\ell(w)$.

Decisive calculation

Repeat with different admissible probes. A useful graph has a stable link backbone and predicts response to probes not used in its construction.

READER CHECK

Given $w_{ab} = 0.8$, $w_{bc} = 0.3$, and threshold 0.5, draw the retained graph.

Graph distance and dimension

DERIVED

Compact equation

$$d_G(a,b) = \min_{\gamma:a\to b} \sum_{e\in\gamma} \ell_e, \qquad d_s = -2\frac{\mathrm{d}\ln P}{\mathrm{d}\ln\sigma}$$

FIRST LOOK

Distance comes from route cost; dimension comes from how diffusion spreads and returns.

Dependency: F05, a positive edge-length map, and graph diffusion.

F06 Working page: Graph distance and dimension

Derivation or construction

Set $\ell_{ab} = \ell_0 f(w_{ab})$ with fixed monotone f. Construct $\mathsf{L} = D - W$ and $K(\sigma) = \mathrm{e}^{-\sigma \mathsf{L}}$. Average the return probability and differentiate its log slope.

Dimensions and normalization

ℓ_0 supplies length. P and d_s are dimensionless; σ is normalized to the Laplacian convention.

Decisive calculation

Look for a broad d_s plateau shared by diffusion, volume growth, and wave propagation. Quantify anisotropy across directions and graph ensembles.

READER CHECK

If $P(\sigma) = 3\sigma^{-3/2}$, calculate $d_s = 3$.

Finite local transition capacity

PROPOSED

Compact equation

$$C_i = \frac{D_i}{D_{\star,i}} \le 1, \qquad r_i = 1 - C_i$$

FIRST LOOK

Every local junction has a finite change budget. Busy regions alter nearby evolution through the same local rule.

Dependency: F01 locality and a nonnegative demand functional.

F07 Working page: Finite local transition capacity

Derivation or construction

Construct D_i from the same variables advanced by the update: amplitude change, phase change, link strain, or rewiring demand. Normalize by a fixed local capacity $D_{\star,i}$.

Dimensions and normalization

The numerator and denominator have identical dimensions, so C_i and r_i are dimensionless. Terms inside D_i must be mutually commensurate.

Decisive calculation

Stress the lattice at increasing load. Record onset, conservation residuals, propagation of saturation, and dependence on boundary size.

READER CHECK

For $D_i = 0.72D_\star$, compute C_i and r_i.

Admissible deterministic update

PROPOSED

Compact equation

$$(X_{n+1}, X_n) = U_p(X_n, X_{n-1}), \qquad U_p(\mathcal{A}) \subseteq \mathcal{A}$$

FIRST LOOK

A complete rule says which legal move happens next and keeps every local demand within capacity.

Dependency: F07 admissible set plus fixed parameters and boundary conditions.

F08 Working page: Admissible deterministic update

Derivation or construction

Prove single-valuedness, then closure by induction on n. Derive exact conserved charges or a declared Lyapunov inequality. Treat graph-change branches and ties explicitly.

Dimensions and normalization

U_p maps like-dimensioned states. Each component of p has a unit or dimensionless normalization.

Decisive calculation

Adversarially sample states near every capacity boundary. Verify closure, locality radius, conservation, stability, and reproducibility across execution order.

READER CHECK

Write one example of an ambiguous tie and a deterministic tie-break that depends only on local state.

D01

BENCHMARK

Discrete graph action

DEFINED

Compact equation

$$S_d = \sum_n \Delta\tau \left[\frac{\mu}{2} \left\| \frac{q^{n+1} - q^n}{\Delta\tau} \right\|^2 - \frac{\kappa}{2a^2} q^{n\mathsf{T}} \mathsf{L} q^n - \sum_i V(q_i^n) \right]$$

FIRST LOOK

The action balances change from one update to the next against link strain and onsite energy.

Dependency: A fixed weighted graph phase and scalar node coordinates.

D01 Working page: Discrete graph action

Derivation or construction

Insert Equation (7.3) to show that the link term equals the sum of squared neighbour differences. The discrete time sum approximates an integral when the clock map and refinement limit exist.

Dimensions and normalization

The bracket has energy dimensions: $[\mu q^2/\Delta\tau^2] = [\kappa q^2/a^2] = [V]$. Multiplication by $\Delta\tau$ gives action.

Decisive calculation

Evaluate the action on a constant configuration, one-node bump, and plane wave. Compare signs and scaling with amplitude.

READER CHECK

Why does the constant mode have zero link energy on a connected graph?

D02

BENCHMARK

Discrete Euler–Lagrange update

DERIVED

Compact equation

$$\mu \frac{q_i^{n+1} - 2q_i^n + q_i^{n-1}}{\Delta\tau^2} = -\frac{\kappa}{a^2}(\mathsf{L}q^n)_i - V'(q_i^n)$$

FIRST LOOK

The next value is determined by the previous two values and the force at the present value.

Dependency: D01 and differentiable onsite potential.

D02 Working page: Discrete Euler–Lagrange update

Derivation or construction

Differentiate the $n-1$ and n kinetic terms with respect to q_i^n. Add the link derivative $-(\kappa/a^2)(\mathsf{L}q^n)_i$ and onsite derivative $-V'(q_i^n)$, then solve for q_i^{n+1}.

Dimensions and normalization

Both sides have force-like dimensions $[\mu q/T^2]$.

Decisive calculation

Compare analytic gradients of S_d with finite-difference gradients on random small graphs.

READER CHECK

For a free isolated node, show that the update gives $q^{n+1} - q^n = q^n - q^{n-1}$: constant discrete velocity.

D03

BENCHMARK

Weighted graph Laplacian

DERIVED

Compact equation

$$(\mathsf{L}q)_i = \sum_j w_{ij}(q_i - q_j), \qquad q^{\mathsf{T}}\mathsf{L}q = \frac{1}{2}\sum_{ij} w_{ij}(q_i - q_j)^2$$

FIRST LOOK

The Laplacian compares each value with a weighted neighbour average and produces the restoring link force.

Dependency: Symmetric nonnegative weights.

D03 Working page: Weighted graph Laplacian

Derivation or construction

Expand the quadratic form. Symmetry makes the two q_i^2 sums equal, leaving $q^{\mathsf{T}}(D - W)q$. Positivity follows term by term.

Dimensions and normalization

w_{ij} is dimensionless in the benchmark; κ/a^2 carries the physical stiffness normalization.

Decisive calculation

Diagonalize L. Require nonnegative eigenvalues and one zero eigenvalue per connected component.

READER CHECK

Compute the Laplacian matrix of a three-node path and verify its row sums are zero.

Deterministic recursion theorem

DERIVED

Compact equation

$$q^{n+1} = 2q^n - q^{n-1} - \frac{\Delta\tau^2}{\mu}\left(\frac{\kappa}{a^2}\mathsf{L}q^n + V'(q^n)\right)$$

FIRST LOOK

Once two consecutive states are known, ordinary arithmetic gives exactly one next benchmark state.

Dependency: D02, finite graph, $\mu > 0$, and single-valued V'.

D04 Working page: Deterministic recursion theorem

Derivation or construction

The graph Laplacian is a finite matrix. Every vector operation on the right is single-valued. Division by positive μ is defined. Therefore the recursion gives a unique real vector.

Dimensions and normalization

The coefficient $\Delta\tau^2/\mu$ converts force to coordinate increment.

Decisive calculation

Run two independent implementations from byte-identical inputs and compare every output bit or declared tolerance.

READER CHECK

List which inputs must be stored to reproduce update 100 without ambiguity.

Discrete energy ledger

DERIVED

Compact equation

$$H^{n+1/2} = \frac{1}{2}\left\|\frac{q^{n+1} - q^n}{\Delta\tau}\right\|^2 + \frac{1}{2}(q^{n+1})^\mathsf{T} A q^n$$

FIRST LOOK

The linear central update carries an exact step-to-step balance that can be checked numerically.

Dependency: Linear harmonic benchmark with symmetric A.

D05 Working page: Discrete energy ledger

Derivation or construction

Subtract consecutive half-step expressions. Factor $q^{n+1} - q^{n-1}$ and use $q^{n+1} - 2q^n + q^{n-1} = -\Delta\tau^2 A q^n$. Symmetry cancels the remaining terms.

Dimensions and normalization

As written, H is normalized per unit inertia. Multiply by μ for benchmark energy dimensions.

Decisive calculation

Track $H^{n+1/2}$ over long stable runs. Report maximum relative drift and scaling with floating-point precision.

READER CHECK

Verify the invariant for one oscillator over the first two updates by direct substitution.

Local proposal limiter

PROPOSED

Compact equation

$$q_i^{n+1} = q_i^n + \eta_i(\tilde{q}_i^{n+1} - q_i^n), \qquad 0 \le \eta_i \le 1$$

FIRST LOOK

When an unconstrained move asks too much of a node, a local factor shortens that move.

Dependency: D02 proposal and F07 demand.

D06 Working page: Local proposal limiter

Derivation or construction

Compute $\tilde{q}^{,n+1}$ from the benchmark. Solve the local inequality $C_i(\eta_i) \leq 1$ for the largest admissible factor, including coupled neighbour constraints by a deterministic local iteration.

Dimensions and normalization

η_i is dimensionless. The demand inequality carries the units.

Decisive calculation

Map capacity violations, energy residuals, and propagation speed as the load crosses threshold.

READER CHECK

If kinetic demand alone scales as η^2 and the proposal has $C = 1.44$, find $\eta = 1/\sqrt{1.44} = 5/6$.

Capacity projection

PROPOSED

Compact equation

$$X_{n+1} = \operatorname*{argmin}_{Y \in \mathcal{A}_{\text{local}}} \left\| Y - \widetilde{X}_{n+1} \right\|_M^2$$

FIRST LOOK

Choose the closest admissible local state according to a fixed metric, with a fixed rule for equal minima.

Dependency: D06, a convex or otherwise well-specified admissible set, and metric M.

D07 Working page: Capacity projection

Derivation or construction

Formulate the local constrained optimization, include conserved linear charges as equality constraints, and prove existence and uniqueness under the chosen geometry. If the set is not convex, specify deterministic branch selection.

Dimensions and normalization

The metric M normalizes unlike coordinates so the squared distance is dimensionless or has one declared unit.

Decisive calculation

Compare the projected change with an independently integrated constrained dynamics. Check closure and charge balance at every saturated node.

READER CHECK

Project the scalar proposal $y = 1.3$ onto interval $[-1, 1]$ under Euclidean distance. The answer is 1.

D08

BENCHMARK

Continuum scaling

DERIVED

Compact equation

$$q_i = a^{d/2}\phi(x_i), \qquad \sum_i q_i^2 \to \int \phi^2 \,\mathrm{d}^d x$$

FIRST LOOK

The field is normalized so a sum over nodes becomes an integral over space.

Dependency: D01 and a regular graph phase with cell volume a^d.

D08 Working page: Continuum scaling

Derivation or construction

Insert the normalization, Taylor-expand neighbour differences, and replace $\sum_i a^d$ by $\int \mathrm{d}^d x$. Keep the leading a^2 correction to measure convergence.

Dimensions and normalization

a carries length after metric matching. The field dimension follows from the canonical continuum kinetic term.

Decisive calculation

Repeat one fixed physical wave packet at $a, a/2, a/4$ and estimate order by Equation (20.8).

READER CHECK

Show that $\sum_i q_i^2$ is unchanged in the continuum normalization when the number of cells doubles in each dimension and a halves.

Plane-wave eigenmodes

DERIVED

Compact equation

$$q_{\mathbf{j}}^{,n} = A\mathrm{e}^{\mathrm{i}(\mathbf{k}\cdot\mathbf{x}_{\mathbf{j}}-\omega n\Delta\tau)}$$

FIRST LOOK

A plane wave repeats the same phase pattern across a periodic regular lattice.

Dependency: D02 on a translation-invariant graph.

S01 Working page: Plane-wave eigenmodes

Derivation or construction

Shift the lattice index by one cell; the mode acquires factor $e^{ik_r a}$. Translation invariance makes it a simultaneous eigenvector of all shift operators and hence of the Laplacian.

Dimensions and normalization

k has inverse-length dimensions after a is matched; ω has inverse-time dimensions after $\Delta\tau$ is matched.

Decisive calculation

Initialize one exact mode and measure leakage into all other discrete Fourier components.

READER CHECK

For a chain of N periodic nodes, list allowed $k_m = 2\pi m/(Na)$.

Exact lattice dispersion

DERIVED

Compact equation

$$\frac{4}{\Delta\tau^2}\sin^2\frac{\omega\Delta\tau}{2} = \Omega_0^2 + \frac{4c^2}{a^2}\sum_r \sin^2\frac{k_r a}{2}$$

FIRST LOOK

The equation tells every represented wavelength exactly how fast its phase advances per update.

Dependency: S01, harmonic onsite potential, and cubic periodic lattice.

S02 Working page: Exact lattice dispersion

Derivation or construction

Evaluate the temporal second difference and spatial Laplacian eigenvalue separately; cancel the nonzero plane-wave amplitude.

Dimensions and normalization

Every term has dimensions T^{-2}. The sine arguments are dimensionless.

Decisive calculation

Compare fitted mode frequencies with the analytic inverse-sine expression over the whole Brillouin zone.

READER CHECK

Set $k = 0$. Show that the frequency is the lattice gap determined by Ω_0.

Long-wavelength expansion

DERIVED

Compact equation

$$\omega^2 = \Omega_0^2 + c^2k^2 + \frac{\Delta\tau^2\omega^4}{12} - \frac{c^2a^2}{12}\sum_r k_r^4 + \cdots$$

FIRST LOOK

Long waves forget much of the lattice, while the first corrections remember spacing and direction.

Dependency: S02 and small $|k_r a|$, $|\omega\Delta\tau|$.

S03 Working page: Long-wavelength expansion

Derivation or construction

Use $\sin^2(x/2) = x^2/4 - x^4/48 + \mathcal{O}(x^6)$ on both sides of the exact dispersion relation.

Dimensions and normalization

Each correction has dimensions T^{-2}. Directional $\sum k_r^4$ differs from rotational $(k^2)^2$ and measures anisotropy.

Decisive calculation

Fit simulated residuals to $a^2 \sum k_r^4$ and $\Delta\tau^2\omega^4$ on refinements.

READER CHECK

Compare waves with $\mathbf{k} = (k, 0, 0)$ and $(k/\sqrt{3}, k/\sqrt{3}, k/\sqrt{3})$; calculate which has larger $\sum k_r^4$.

Group velocity and causal cone

DERIVED

Compact equation

$$v_{g,r} = \frac{(c^2/a)\sin(k_r a)}{\sqrt{A(\mathbf{k})}\sqrt{1-\Delta\tau^2 A(\mathbf{k})/4}}$$

FIRST LOOK

A packet moves at the slope of the frequency band, not generally at the phase speed of one crest.

Dependency: S02 within the stable domain.

S04 Working page: Group velocity and causal cone

Derivation or construction

Solve for $\omega(\mathbf{k})$ with an inverse sine and differentiate. The chain rule supplies $\partial A/\partial k_r = (2c^2/a)\sin(k_r a)$.

Dimensions and normalization

$\partial\omega/\partial k$ has dimensions length/time.

Decisive calculation

Launch narrow-band packets and compare measured envelope speed with the analytic derivative. Test direction dependence.

READER CHECK

For massless long waves, insert $A \approx c^2 k^2$ and show $|\mathbf{v}_g| \to c$.

Courant stability domain

DERIVED

Compact equation

$$\Delta\tau^2 \left(\Omega_0^2 + \frac{4dc^2}{a^2}\right) \leq 4$$

FIRST LOOK

The time step must be short enough to resolve the fastest lattice mode.

Dependency: S02 and all normal modes of the linear benchmark.

S05 Working page: Courant stability domain

Derivation or construction

Require the inverse-sine argument to be at most one. Maximize the spatial sine sum at a Brillouin-zone corner, where it equals d.

Dimensions and normalization

The bracket has T^{-2}, so the product is dimensionless.

Decisive calculation

Sweep across the boundary at fixed graph size. Fit the growth exponent of the corner mode.

READER CHECK

For $d = 1$, $a = c = 1$, and $\Omega_0 = 0$, find $\Delta\tau \leq 1$.

Mass gap

DERIVED

Compact equation

$$m_{\text{eff}} = \frac{\hbar\omega_0}{c_{\text{phys}}^2}$$

FIRST LOOK

A nonzero lowest frequency costs energy even when the pattern has no spatial momentum.

Dependency: S02 at $\mathbf{k} = 0$, plus matched $\hbar$ and physical causal speed.

S06 Working page: Mass gap

Derivation or construction

Find ω_0 from the exact lattice gap. In the relativistic low-energy dictionary set rest energy $E_0 = \hbar\omega_0 = mc^2$.

Dimensions and normalization

$\hbar\omega_0$ is energy; division by speed squared gives mass.

Decisive calculation

Identify multiple stable patterns without target masses. Compare their dimensionless gap ratios on refinements.

READER CHECK

If $\omega_a = 3\omega_b$, show that $m_a/m_b = 3$ after the common dictionary cancels.

Nonlinear frequency shift

DERIVED

Compact equation

$$\Omega(A) \approx \Omega_0 \left(1 + \frac{3\lambda A^2}{8\mu\Omega_0^2}\right)$$

FIRST LOOK

A nonlinear oscillator's clock rate can depend on how strongly it is excited.

Dependency: Duffing equation and weak nonlinearity.

S07 Working page: Nonlinear frequency shift

Derivation or construction

Insert $q = A\cos\Omega t$, use $\cos^3 x = (3\cos x + \cos 3x)/4$, balance the fundamental, and expand the square root.

Dimensions and normalization

$\lambda A^2/(\mu\Omega_0^2)$ is dimensionless.

Decisive calculation

Measure Ω versus A^2 at small amplitude. Compare the fitted slope with $3\lambda/(8\mu\Omega_0)$.

READER CHECK

For positive λ, decide whether frequency increases or decreases with amplitude.

Localized nonlinear modes

PROPOSED

Compact equation

$$\left[\Omega_0^2 I + \frac{\kappa}{\mu a^2}\mathsf{L} - \Omega^2 I\right]\phi + \frac{3\lambda}{4\mu}\phi^{\circ 3} = 0$$

FIRST LOOK

Nonlinearity can balance dispersion and hold a vibrating pattern near a small set of nodes.

Dependency: S07 on a graph, harmonic balance, and a localization search.

S08 Working page: Localized nonlinear modes

Derivation or construction

Use an anti-continuum seed or constrained Newton solve. Continue coupling, compute participation ratio, and linearize one period for Floquet multipliers.

Dimensions and normalization

Normalize ϕ by a fixed norm; report frequencies and amplitudes in dimensionless benchmark units before physical matching.

Decisive calculation

Perturb each candidate, vary graph size and boundary conditions, and publish the region where it persists.

READER CHECK

For a vector supported equally on m nodes and zero elsewhere, show that its participation ratio is m.

Complex node field

DEFINED

Compact equation

$$\psi_i = \rho_i e^{i\theta_i}, \qquad \theta_i \sim \theta_i + 2\pi$$

FIRST LOOK

Amplitude says how much; phase says where the local cycle sits.

Dependency: D01 extended from a real coordinate to a complex coordinate.

G01 Working page: Complex node field

Derivation or construction

Write real and imaginary parts or polar variables. Require observables to be insensitive to the chosen 2π representative. Treat $\rho = 0$ separately because phase is undefined there.

Dimensions and normalization

θ is dimensionless. The normalization and mass dimension of ρ follow the chosen action.

Decisive calculation

Evolve a global phase-rotated initial state and compare all invariant observables.

READER CHECK

Show that $|\rho \mathrm{e}^{\mathrm{i}(\theta+2\pi)}|^2 = \rho^2$.

Covariant link difference

DEFINED

Compact equation

$$D_{ij}\psi = U_{ij}\psi_j - \psi_i, \qquad U_{ji} = U_{ij}^{-1}$$

FIRST LOOK

Before comparing phases at different nodes, transport one phase along the link.

Dependency: G01 and compact link transporter.

G02 Working page: Covariant link difference

Derivation or construction

Assign $U_{ij} \in U(1)$ to each orientation. The difference reduces to $\psi_j - \psi_i$ in gauge $U_{ij} = 1$. Reverse orientation by group inverse.

Dimensions and normalization

U_{ij} and the link exponent are dimensionless. $D_{ij}\psi$ has the same dimensions as ψ.

Decisive calculation

Verify covariance under thousands of random local phase transformations.

READER CHECK

If $U_{ij} = \mathrm{e}^{\mathrm{i}\pi/2}$ and $\psi_j = 1$, $\psi_i = \mathrm{i}$, calculate $D_{ij}\psi = 0$.

Local gauge transformation

DERIVED

Compact equation

$$\psi_i' = \mathrm{e}^{\mathrm{i}q\alpha_i}\psi_i, \qquad U_{ij}' = \mathrm{e}^{\mathrm{i}q\alpha_i}U_{ij}\mathrm{e}^{-\mathrm{i}q\alpha_j}$$

FIRST LOOK

Each node may choose its own phase reference; link variables compensate so physics stays unchanged.

Dependency: G02.

G03 Working page: Local gauge transformation

Derivation or construction

Substitute the transformed objects into $D'_{ij}\psi'$ and factor out $\mathrm{e}^{\mathrm{i}q\alpha_i}$. Absolute squares and closed loops are invariant.

Dimensions and normalization

$q\alpha_i$ is dimensionless. The split between q and A_{ij} depends on charge normalization.

Decisive calculation

Randomize α_i and compare action terms, currents, and loop products at floating-point tolerance.

READER CHECK

Perform the three-line cancellation leading to Equation (12.8).

Plaquette holonomy

DERIVED

Compact equation

$$U_\square = \prod_{(ij)\in\partial\square} U_{ij}$$

FIRST LOOK

Transport around a closed elementary loop. The leftover phase records gauge curvature.

Dependency: G03 and an oriented plaquette.

G04 Working page: Plaquette holonomy

Derivation or construction

Multiply the transformed links in order. Every node factor appears once with positive and once with negative exponent, so they cancel. Reverse the loop to obtain $U_\square^{-1}$.

Dimensions and normalization

$U_\square$ is dimensionless. In a smooth limit its phase is $qa^2F_{\mu\nu} + \cdots$.

Decisive calculation

Compare loop products before and after gauge transformation; then test the area scaling of small smooth fields.

READER CHECK

Write the cancellation explicitly for a four-link square.

Gauge-field action

PROPOSED

Compact equation

$$S_g = -\frac{\beta}{a^4} \sum_{n,\square} \Delta\tau \left(1 - \mathrm{Re}\, U_\square^n\right)$$

FIRST LOOK

The action penalizes loop phase mismatch while preserving exact local gauge symmetry.

Dependency: G04 and a declared lattice normalization.

G05 Working page: Gauge-field action

Derivation or construction

Use $1 - \cos \Phi_{\square}$ as the compact local curvature energy. Expand for small $\Phi_{\square}$ to recover a quadratic field-strength term.

Dimensions and normalization

β/a^4 and the spacetime cell measure must combine to action dimensions; conventions differ between Euclidean and real-time formulations.

Decisive calculation

Unit-test gauge invariance and compare small-field dispersion with the intended continuum gauge sector.

READER CHECK

Expand $1 - \cos x = x^2/2 + \mathcal{O}(x^4)$.

Continuum gauge coupling

PROPOSED

Compact equation

$$1 - \mathrm{Re}\, U_{\square} \approx \frac{1}{2} q^2 a^4 F_{\mu\nu} F^{\mu\nu}$$

FIRST LOOK

A measured low-energy coupling comes from the normalization and renormalization of the lattice link sector.

Dependency: G05, matter content, regulator, and continuum limit.

G06 Working page: Continuum gauge coupling

Derivation or construction

Match the expanded plaquette action to $-F^2/(4g^2)$ in a declared convention. Compute correlation functions and run the coupling to the comparison scale.

Dimensions and normalization

g is dimensionless in four spacetime dimensions; bare and renormalized couplings carry scale and scheme labels.

Decisive calculation

Predict coupling flow at a held-out scale after fixing the bare model on calibration observables.

READER CHECK

Explain why inserting the measured α into the bare charge and recovering it later is calibration.

Charge representations

PROPOSED

Compact equation

$$\psi_i \mapsto R(g_i)\psi_i, \qquad U_{ij} \mapsto R(g_i)U_{ij}R(g_j)^{-1}$$

FIRST LOOK

Different pattern types may transform in different representations of the same local symmetry.

Dependency: G03 generalized to a declared group.

G07 Working page: Charge representations

Derivation or construction

Identify stable pattern multiplets and compute how link transport acts on their internal state space. The generators and representation weights define charges.

Dimensions and normalization

Charge labels are dimensionless representation data; physical coupling strength belongs to the action normalization.

Decisive calculation

Derive conserved lattice currents and verify charge addition in scattering states.

READER CHECK

For $U(1)$, show that charges q_1 and q_2 make a product field transform with charge $q_1 + q_2$.

Chiral fermion hurdle

TEST

Compact equation

$$\{\gamma_5, D\} = 0 \quad \text{and} \quad \text{locality, translation symmetry, no doubling}$$

FIRST LOOK

Left- and right-handed matter cannot be placed naively on a regular lattice without extra states or a refined construction.

Dependency: G07 plus a fermionic node operator.

G08 Working page: Chiral fermion hurdle

Derivation or construction

State which hypothesis of the Nielsen–Ninomiya theorem is modified by the construction: operator relation, locality notion, lattice regularity, boundary/domain-wall structure, or another explicit mechanism.

Dimensions and normalization

Fermion fields have mass dimension $3/2$ in four-dimensional continuum normalization.

Decisive calculation

Compute the full low-energy spectrum, chirality, anomaly coefficients, and unwanted mirror modes on refinements.

READER CHECK

State the difference between a Dirac mass coupling left and right components and a purely chiral gauge representation.

Conservative amplitude–phase action

PROPOSED

Compact equation

$$\mathcal{L} = \tfrac{1}{2}(\partial\Phi)^2 + \tfrac{1}{2}f_\theta^2(\Phi)(\partial\theta)^2 - U(\Phi) - \tfrac{\eta}{2}(\Box\Phi)^2$$

FIRST LOOK

Amplitude and phase can share one effective field action, with every sign and derivative order displayed.

Dependency: G01 continuum field plus a stated effective regime.

L01 Working page: Conservative amplitude–phase action

Derivation or construction

Write $\Psi = \Phi e^{i\theta}$. The ordinary kinetic identity $|\partial\Psi|^2 = (\partial\Phi)^2 + \Phi^2(\partial\theta)^2$ motivates $f_\theta(\Phi) = \Phi$ in the simplest case. Higher derivatives are kept as separate effective operators.

Dimensions and normalization

In four dimensions $[\Phi] = [f_\theta] = M$, $[U] = M^4$, and $[\eta] = M^{-2}$ in natural units.

Decisive calculation

Derive the quadratic propagator around each background. Check pole signs, gradient stability, and the scale below which the derivative expansion is valid.

READER CHECK

Expand $|\partial(\Phi e^{i\theta})|^2$ and show the cross terms cancel.

Link phase mismatch

DERIVED

Compact equation

$$|U_{ij}\psi_j - \psi_i|^2 = \rho_i^2 + \rho_j^2 - 2\rho_i\rho_j\cos(\theta_j - \theta_i + qA_{ij})$$

FIRST LOOK

A link stores energy when neighbouring transported phases fail to align.

Dependency: G01–G03.

L02 Working page: Link phase mismatch

Derivation or construction

Insert polar forms and multiply by the complex conjugate. The real part of $\mathrm{e}^{\mathrm{i}(\theta_j-\theta_i+qA_{ij})}$ produces the cosine.

Dimensions and normalization

The squared mismatch has the square of the field amplitude's units. The cosine argument is dimensionless.

Decisive calculation

Compare the expanded small-mismatch form with a phase-stiffness action and measure nonlinear phase slips.

READER CHECK

Set equal amplitudes ρ and small mismatch δ. Use $1-\cos\delta \approx \delta^2/2$.

Positivity and derivative order

TEST

Compact equation

$$K_{AB}\dot{\varphi}^A\dot{\varphi}^B > 0, \qquad \det K \neq 0$$

FIRST LOOK

The kinetic matrix must assign positive energy to ordinary small disturbances in its domain of use.

Dependency: L01 expanded about a specified background.

L03 Working page: Positivity and derivative order

Derivation or construction

Compute the Hessian of the Lagrangian with respect to time derivatives. Diagonalize K_{AB}. Treat higher-time-derivative terms through their declared effective cutoff or a degenerate constrained construction.

Dimensions and normalization

Eigenvalues of K share the normalization needed to make kinetic energy density. Rescale fields only with a recorded Jacobian.

Decisive calculation

Scan backgrounds and momenta below the cutoff for ghost, gradient, and tachyonic instabilities.

READER CHECK

For $K = \begin{pmatrix} 2 & 1 \\ 1 & 2 \end{pmatrix}$, calculate eigenvalues 1 and 3, both positive.

Residual capacity

DEFINED

Compact equation

$$r_i^n = 1 - C_i^n, \qquad 0 \le r_i^n \le 1$$

FIRST LOOK

Residual capacity is the unused fraction of one node's local change budget.

Dependency: F07 local demand.

C01 Working page: Residual capacity

Derivation or construction

Normalize the nonnegative demand by a fixed capacity. Subtract from one. Keep the ledger local; regional residual is a sum over a declared finite region.

Dimensions and normalization

C_i and r_i are dimensionless. A continuum field normalization is a later construction.

Decisive calculation

Record the distribution and correlation length of r_i as load changes.

READER CHECK

If three nodes have $C = (0.2, 0.7, 1.0)$, compute $r = (0.8, 0.3, 0)$.

Causal capacity balance

PROPOSED

Compact equation

$$r_i^{n+1} - r_i^n + \sum_j J_{ij}^n = s_i^n, \qquad J_{ij} = -J_{ji}$$

FIRST LOOK

Residual capacity may move through links or change through a declared local source.

Dependency: C01 and an oriented link-current rule.

C02 Working page: Causal capacity balance

Derivation or construction

Sum the local equations over a region. Antisymmetric internal currents cancel, leaving boundary flux and local sources as in Equation (16.2).

Dimensions and normalization

Every term is residual fraction per update. Multiply by a local capacity and divide by clock step for physical power-like units.

Decisive calculation

Inject a localized source and measure finite-speed spreading, boundary balance, and dependence on update order.

READER CHECK

Show explicitly that $J_{12} + J_{21} = 0$ cancels inside a two-node region.

Coarse EQEF field

PROPOSED

Compact equation

$$\chi_R(x) = Z_R \sum_i K_R(x,i)(r_i - \bar{r})$$

FIRST LOOK

Average local residual fluctuations into a smooth field at resolution R.

Dependency: C01–C02 and a normalized coarse kernel.

C03 Working page: Coarse EQEF field

Derivation or construction

Choose $\sum_i K_R(x, i) = 1$. Subtract the background and select Z_R so the two-point function has a stable continuum normalization.

Dimensions and normalization

r_i is dimensionless; Z_R supplies the continuum field dimension. State it before writing the action.

Decisive calculation

Measure $\langle \chi(x)\chi(y) \rangle$, dispersion, and response to a known capacity source over refinements.

READER CHECK

If a kernel averages four equal weights and residual deviations are $(.2, .1, -.1, -.2)$, show $\chi/Z_R = 0$.

Response and source map

PROPOSED

Compact equation

$$\frac{\delta\langle\chi(x)\rangle}{\delta s(y)} = G_{\chi s}(x, y)$$

FIRST LOOK

A field earns physical meaning through how it responds to a controlled source.

Dependency: C03 plus an intervention that changes local demand.

C04 Working page: Response and source map

Derivation or construction

Perturb $s(y)$ by a small impulse. Average repeated trajectories or spatially equivalent trials. The linear response kernel is the functional derivative of the mean field.

Dimensions and normalization

$G_{\chi s}$ carries the field units divided by source units. Fourier poles define propagation and damping scales.

Decisive calculation

Compare the measured response kernel with the one derived from Equation (16.4).

READER CHECK

For a linear oscillator response $G(\omega) = 1/(m^2 - \omega^2)$, locate its poles.

Torsion from loop nonclosure

PROPOSED

Compact equation

$$\Delta x^{\mu} = T^{\mu}_{\nu\rho} u^{\nu} v^{\rho} + \cdots$$

FIRST LOOK

If two transport orders end at different coarse positions, their small-loop mismatch defines a torsion candidate.

Dependency: F05–F06 geometry and a derived transport law.

C05 Working page: Torsion from loop nonclosure

Derivation or construction

Transport a localized probe around both orders of a small loop. Convert endpoint pattern difference through the coarse position map. Divide by oriented area and take the refinement limit.

Dimensions and normalization

$T^{\mu}_{\nu\rho}$ has inverse-length dimensions in a coordinate basis. The loop mismatch has length.

Decisive calculation

Check tensor transformation, orientation reversal, universality across probes, and scaling with loop area.

READER CHECK

Reverse u and v in Equation (15.4); show the leading mismatch changes sign because torsion is antisymmetric in the last two indices.

Tetrad and connection bridge

PROPOSED

Compact equation

$$T^a = \mathrm{d}e^a + \omega^a{}_b \wedge e^b, \qquad R^a{}_b = \mathrm{d}\omega^a{}_b + \omega^a{}_c \wedge \omega^c{}_b$$

FIRST LOOK

A tetrad converts local frame readings into spacetime intervals; a connection compares frames at neighbouring points.

Dependency: C05 plus clocks, rods, and orientation observables.

C06 Working page: Tetrad and connection bridge

Derivation or construction

Build local orthonormal response modes, define $e^a{}_\mu$ from their calibrated intervals, and infer ω from transport. Compute torsion and curvature as exterior field strengths.

Dimensions and normalization

$e^a{}_\mu$ depends on coordinate conventions; ω and torsion carry inverse-length scale after physical matching.

Decisive calculation

Reconstruct the same geometry with independent clock and probe species. Quantify non-universal residuals.

READER CHECK

Use $g_{\mu\nu} = \eta_{ab} e^a{}_\mu e^b{}_\nu$ to show that a local Lorentz rotation leaves g invariant.

Emergent metric

PROPOSED

Compact equation

$$g^{\mu\nu}(x)k_\mu k_\nu = 0$$

FIRST LOOK

The common wavefront relation of several light sectors defines the effective causal geometry.

Dependency: F03 clocks, F06 distance, and continuum wave modes.

R01 Working page: Emergent metric

Derivation or construction

Fit local dispersion surfaces to a quadratic form in covectors. Normalize with one clock/rod convention and compare the resulting metric across sectors.

Dimensions and normalization

k_μ has inverse-coordinate units; $g^{\mu\nu}$ carries the corresponding conversion so the eikonal equation is homogeneous.

Decisive calculation

Test one common metric against held-out wave directions, polarizations, frequencies, and matter species.

READER CHECK

For flat space, insert $g^{\mu\nu} = \mathrm{diag}(-1/c^2, 1, 1, 1)$ and derive $\omega^2 = c^2 k^2$.

Equivalence-principle target

TEST

Compact equation

$$\frac{m_g}{m_i} = 1 + \eta_{\text{comp}}, \qquad \eta_{\text{comp}} \to 0$$

FIRST LOOK

Different stable patterns should fall alike when size, spin, and tidal corrections are controlled.

Dependency: R01 and pattern inertial/gravitational response maps.

R02 Working page: Equivalence-principle target

Derivation or construction

Define inertial mass from acceleration under a calibrated non-gravitational force and gravitational charge from response to the emergent potential. Compare ratios across compositions.

Dimensions and normalization

η_{comp} is dimensionless and is the clean universality diagnostic.

Decisive calculation

Simulate or measure differential acceleration with one frozen graph/capacity model and publish the maximum composition residual.

READER CHECK

If two accelerations are a_1 and a_2, write the Eötvös ratio $2|a_1 - a_2|/(|a_1 + a_2|)$.

Newtonian limit

PROPOSED

Compact equation

$$\nabla^2\Phi_N = 4\pi G\rho, \qquad g_{00} \approx -(1 + 2\Phi_N/c^2)$$

FIRST LOOK

A weak, slowly varying source should produce the familiar inverse-distance potential.

Dependency: R01–R02 and a coarse source density.

R03 Working page: Newtonian limit

Derivation or construction

Linearize the derived geometric equations about a homogeneous background. Identify the scalar potential in g_{00} and solve the static response to localized density.

Dimensions and normalization

G has dimensions $L^3M^{-1}T^{-2}$. The source and potential units must reproduce $\nabla^2\Phi$.

Decisive calculation

Fit the same G to multiple source shapes and distances, then test a held-out geometry and composition.

READER CHECK

Integrate the spherical vacuum equation and recover $\Phi = -GM/r$.

Einstein-sector matching

PROPOSED

Compact equation

$$S_g = \frac{c^3}{16\pi G}\int R\sqrt{-g}\,\mathrm{d}^4x + S_{\mathrm{corr}}$$

FIRST LOOK

The long-distance geometry needs one universal curvature response plus calculable corrections.

Dependency: C06 and R01–R03.

R04 Working page: Einstein-sector matching

Derivation or construction

Integrate out short graph modes or match long-wave response functions. Identify the coefficient of R, list all symmetry-allowed corrections, and compute their suppression scales.

Dimensions and normalization

c^3/G times $R\,\mathrm{d}^4x$ has action dimensions in SI. Never mix this coefficient with a natural-unit expression without conversion.

Decisive calculation

Recover post-Newtonian observables, wave polarizations and speed, and the same matter coupling from one coefficient set.

READER CHECK

Vary $\sqrt{-g}R$ formally and state the resulting Einstein tensor term $G_{\mu\nu}$.

Homogeneous cosmology

PROPOSED

Compact equation

$$H^2 = \frac{8\pi G}{3}\rho_{\text{total}} - \frac{k}{a_{\text{cos}}^2} + \frac{\Lambda}{3}$$

FIRST LOOK

Average the derived fields on large scales and calculate how the cosmic scale factor evolves.

Dependency: R04 plus derived matter/EQEF stress energy and initial conditions.

R05 Working page: Homogeneous cosmology

Derivation or construction

Insert a homogeneous isotropic ansatz into the effective equations. Derive the continuity equations from covariant conservation rather than choosing density histories independently.

Dimensions and normalization

H has inverse-time units. Each term in the Friedmann equation has T^{-2}. Distinguish lattice spacing a from cosmological scale factor $a_{\cos}$.

Decisive calculation

Fit calibration parameters to a declared subset, then predict held-out distances, expansion rates, and age relations with covariance.

READER CHECK

For constant equation of state $p = w\rho$, derive $\rho \propto a_{\cos}^{-3(1+w)}$.

Cosmological perturbations

TEST

Compact equation

$$\delta\ddot{X}_k + A_k(t)\delta\dot{X}_k + B_k(t)\delta X_k = S_k(t)$$

FIRST LOOK

Small ripples around the cosmic background seed observable structure and radiation patterns.

Dependency: R05 and the complete quadratic effective action.

R06 Working page: Cosmological perturbations

Derivation or construction

Expand every field to background plus perturbation, construct gauge-invariant variables, and derive the coupled mode equations and initial-state prescription.

Dimensions and normalization

Power spectra carry the field normalization; quote the dimensionless spectrum $\Delta^2(k) = k^3 P(k)/(2\pi^2)$ where appropriate.

Decisive calculation

Calculate microwave-background and matter spectra with the same frozen background parameters; compare full covariance, not selected peaks.

READER CHECK

If $P(k) \propto k^{n_s-4}$ for curvature conventions, compute the scaling of $\Delta^2(k)$.

Ensemble map

PROPOSED

Compact equation

$$P \longmapsto \mu_P(\mathrm{d}\lambda)$$

FIRST LOOK

A repeatable preparation selects a distribution over complete micro-states, even when each state evolves deterministically.

Dependency: F08 and a laboratory preparation protocol.

Q01 Working page: Ensemble map

Derivation or construction

Specify all controlled variables, uncontrolled environmental variables, and how frequencies over repeated preparations define the measure. State whether settings are statistically independent of λ.

Dimensions and normalization

μ_P is normalized: $\int \mu_P = 1$. Densities inherit inverse units of their coordinates.

Decisive calculation

Generate blind repeated preparations and compare predicted sufficient statistics with empirical distributions.

READER CHECK

For a discrete ensemble with weights $(0.2, 0.3, 0.5)$, verify normalization and calculate the probability of the last two states.

Born-rule target

TEST

Compact equation

$$\Pr(x|a,P) = \int \mathbf{1}[A(a,\lambda) = x]\mu_P(\,\mathrm{d}\lambda) = \mathrm{Tr}(\rho_P E_x^{(a)})$$

FIRST LOOK

The micro-model must reproduce the squared-amplitude outcome frequencies for every declared preparation and measurement.

Dependency: Q01 and a detector outcome map.

Q02 Working page: Born-rule target

Derivation or construction

Derive basin measures or amplification-channel frequencies from μ_P. Compare them with the operator probability for phase, amplitude, and entangled preparations.

Dimensions and normalization

Probabilities are dimensionless and sum to one. Detector efficiencies enter once through the response map.

Decisive calculation

Use held-out measurement bases and multi-outcome positive-operator-valued measurements, not only the basis used to tune the ensemble.

READER CHECK

For state amplitudes $(\sqrt{1/3}, \sqrt{2/3})$, calculate Born probabilities $(1/3, 2/3)$.

Bell–CHSH assumptions

TEST

Compact equation

$$S = |E(a,b) + E(a,b') + E(a',b) - E(a',b')|$$

FIRST LOOK

Entangled correlations diagnose the combined assumptions of local response, setting independence, and ordinary probability structure.

Dependency: Q01–Q02 and spacelike separated response maps.

Q03 Working page: Bell–CHSH assumptions

Derivation or construction

Write the joint distribution and identify the factorization or conditional-independence step used to derive $S \leq 2$. A completion states precisely which mathematical step changes.

Dimensions and normalization

S is dimensionless. Setting and outcome conventions must be identical across theory and data.

Decisive calculation

Reproduce the full correlation curve, marginal distributions, setting statistics, and loophole controls with one parameter set.

READER CHECK

Insert the singlet correlation $E(a, b) = -\cos(a - b)$ at optimal angles and obtain $2\sqrt{2}$.

Operational no-signalling

TEST

Compact equation

$$\sum_y P(x, y|a, b) = \sum_y P(x, y|a, b')$$

FIRST LOOK

Remote setting choices may change correlations but not the local outcome frequency available for signalling.

Dependency: Q03 joint outcome distribution.

Q04 Working page: Operational no-signalling

Derivation or construction

Marginalize the joint distribution over the remote outcome. Prove equality for all permitted settings and preparations, including detector imperfections modeled symmetrically.

Dimensions and normalization

Both sides are probabilities. Compare with uncertainty intervals rather than exact finite-sample equality.

Decisive calculation

Run randomized remote settings and test local marginal invariance with a preregistered statistic.

READER CHECK

Given a 2×2 joint table, sum each row and show how to compare the marginal across two remote settings.

Non-circular derivation protocol

DEFINED

Compact equation

$$D = D_{\text{design}} \cup D_{\text{cal}} \cup D_{\text{test}}, \qquad D_{\text{cal}} \cap D_{\text{test}} = \emptyset$$

FIRST LOOK

Use one set of data to choose the model, another to set permitted scales, and a sealed set to test it.

Dependency: The complete model specification and data provenance.

E01 Working page: Non-circular derivation protocol

Derivation or construction

Record which datum selected every equation, prior, parameter, cut, and unit. Freeze the model card and hash before evaluating the test set.

Dimensions and normalization

Unit definitions are not empirical predictions; matched dimensional scales are calibration inputs.

Decisive calculation

Audit the full dependency graph for any path from the held-out target back into model selection or calibration.

READER CHECK

Classify $m = E/c^2$ after inserting measured E and defined c: it is an identity/conversion.

Dimensionless predictions

TEST

Compact equation

$$R = \frac{\Omega_a}{\Omega_b} = \frac{m_a}{m_b}$$

FIRST LOOK

Ratios cancel a common clock or energy scale and are strong early targets for a new model.

Dependency: Two independently identified stable patterns and a shared physical dictionary.

E02 Working page: Dimensionless predictions

Derivation or construction

Compute both gaps from the frozen micro-model, propagate finite-size and refinement uncertainty, and take the ratio before comparing with particle data.

Dimensions and normalization

R is dimensionless. Common multiplicative scale uncertainty cancels, while correlated numerical errors require covariance.

Decisive calculation

Blind the physical labels during the pattern search, then compare the ranked ratio catalogue with held-out targets using a declared multiplicity correction.

READER CHECK

If gaps are 2.40 ± 0.03 and 1.20 ± 0.02 with zero covariance, calculate $R = 2.00$ and propagate its uncertainty.

Uncertainty and covariance

DERIVED

Compact equation

$$V_y = J V_x J^{\mathsf{T}}, \qquad J_{ij} = \partial f_i / \partial x_j$$

FIRST LOOK

Uncertainty follows the slope of the calculation, and shared inputs make outputs move together.

Dependency: A differentiable output map and input covariance.

E03 Working page: Uncertainty and covariance

Derivation or construction

Linearize $f(x)$ about the central inputs: $\delta y \approx J\delta x$. Take the expectation of $\delta y \delta y^{\mathsf{T}}$. Use Monte Carlo or higher-order methods when nonlinearity is material.

Dimensions and normalization

Covariance entries carry products of output units. Correlation coefficients are dimensionless.

Decisive calculation

Validate propagated intervals with synthetic draws from the full input distribution and measure coverage.

READER CHECK

For $y = x^2$, show $u(y) \approx 2|x|u(x)$ at first order.

Frozen falsification protocol

TEST

Compact equation

$$\hat{y}_{\text{test}} = F(\mathcal{C}_{\text{frozen}}; X_{\text{test}}), \qquad \mathcal{D} = \text{pass or fail rule}$$

FIRST LOOK

A prediction is made by an immutable calculation and judged by a rule written before the answer is seen.

Dependency: E01–E03 and a baseline model.

E04 Working page: Frozen falsification protocol

Derivation or construction

Archive the model card, software environment, data identifiers, checksums, selection, likelihood, and decision threshold. Evaluate once; later revisions receive a new version and a new hold-out.

Dimensions and normalization

The statistic and threshold have declared normalization and sampling distribution.

Decisive calculation

Independent reproduction obtains the same result from the archive and applies the same decision rule.

READER CHECK

Write a one-sentence failure rule for the exact dispersion test that includes a numerical tolerance and wave-number range.

Atlas concordance

Reader goal	Primary codes	Follow next
Understand the ontology	F01–F08	D01–D08 for an executable benchmark
Reproduce exact mathematics	D01–D05, S01–S07, G01–G05	E03 for numerical uncertainty
Develop the capacity mechanism	F07–F08, D06–D07, C01–C04	C05–C06 and R01
Search for particle-like patterns	S06–S08, G07	E01–E04
Build quantum completion	Q01–Q04	Detector maps in Chapter 19
Build gravity/cosmology	C05–C06, R01–R06	Frozen evidence protocol E01–E04
Prepare an empirical test	E01–E04	Chapters 19 and 23

A

Notation and unit discipline

Symbol	Meaning	Discipline
n	micro-update index	Dimensionless order label, not automatically physical time
t_K	clock time	Reading of persistent clock pattern K
X_n	complete micro-state	Contains every variable required by the update
$G = (V, E, W)$	weighted graph	Primitive only in the benchmark; emergent in the full ontology
a	regular-phase link spacing	Length after metric matching; numerical grid scale before it
$\Delta\tau$	benchmark clock step	Time after a clock map; otherwise update parameter
q_i^n	real node coordinate	Normalized so the action terms have common units
ψ_i	complex node field	Amplitude and compact phase
U_{ij}	link transporter	Dimensionless group element; inverse under orientation reversal
L	weighted graph Laplacian	Positive semidefinite for symmetric nonnegative weights
μ	node inertia	$[\mu q^2/T^2] =$ energy
κ	link stiffness parameter	κ/μ sets squared wave speed in the benchmark convention
Ω_0	onsite angular-frequency scale	Inverse time after clock matching
$E_\star$	local capacity scale	Same energy units as local demand
C_i, r_i	demand and residual fractions	Dimensionless and local
χ	coarse EQEF candidate	Normalization and field dimension derived from coarse response
$e^a{}_\mu$	tetrad	Converts coordinate increments to local frame components
$\omega^a{}_b$	spin connection	Compares local frames under transport
$T^a, R^a{}_b$	torsion and curvature	Field strengths of tetrad/connection geometry

A.1 SI and natural units

In SI, c and h have exact defined numerical values and $\hbar = h/(2\pi)$. In natural units one sets $\hbar = c = 1$ as a unit convention. A natural-unit equation is converted only after restoring powers that reproduce the desired SI dimensions.

For example, a mass m written in electronvolts in natural units means the rest energy mc^2 in SI. A cross section in GeV^{-2} requires the conversion

$$1\ \mathrm{GeV}^{-2} = 0.389379 \times 10^{-27}\ \mathrm{cm}^2. \tag{A.1}$$

DRY NOTE FROM THE FLIGHT DECK

Setting $c = 1$ makes the algebra shorter. It does not make a metre equal to a second in the equipment cupboard.

B

Equation audit workbook

Use this six-line audit for every proposed equation.

1. **Types:** What mathematical kind is each symbol: scalar, vector, operator, probability measure, graph, tensor, or group element?
2. **Dimensions:** Do all added terms share dimensions? Are every logarithm, exponential, sine, and phase argument dimensionless?
3. **Dependencies:** Does the equation use only objects constructed earlier in the hierarchy?
4. **Status:** Is it a definition, derived result, matching relation, measured input, or held-out prediction?
5. **Limits:** What happens for zero coupling, constant field, long wavelength, small amplitude, and fine resolution?
6. **Test:** Which calculation or observation changes confidence in the equation?

B.1 Derivative audit

For a derivative $\partial y/\partial x$, check

$$\left[\frac{\partial y}{\partial x}\right] = \frac{[y]}{[x]}. \tag{B.1}$$

For a functional derivative,

$$\delta S = \int \frac{\delta S}{\delta\phi(x)}\delta\phi(x)\,\mathrm{d}^d x, \tag{B.2}$$

so the measure and field variation determine the units of $\delta S/\delta\phi$.

B.2 Matrix audit

Before diagonalizing, verify symmetry or Hermiticity in the correct inner product. For a generalized eigenproblem

$$Ku = \omega^2 M u, \tag{B.3}$$

the mass matrix M defines the inner product. Normalize modes by $u_r^{\mathsf{T}} M u_s = \delta_{rs}$.

B.3 Probability audit

Verify positivity and normalization:

$$P(x) \geq 0, \qquad \sum_x P(x) = 1 \quad \text{or} \quad \int p(x)\,\mathrm{d}x = 1. \tag{B.4}$$

Conditioning variables must be printed. The expressions $P(x)$, $P(x|a)$, and $P(x|a,P)$ are different claims.

C

Problems

The problems progress from direct substitution to research-level design. Answers follow in the next appendix.

Foundations

P1. A clock advances 0.25 rad per update. Calculate updates per cycle.

P2. A persistent pattern has internal period 20 updates and lifetime 2,000 updates. Calculate the number of survived cycles.

P3. If $P(\sigma) = 5\sigma^{-2}$, calculate spectral dimension.

P4. On a graph with edge lengths $\ell_{ab} = 1$, $\ell_{bc} = 2$, and $\ell_{ac} = 4$, find the shortest distance from a to c.

P5. Local demands are $(0.4, 0.9, 1.0)$ of capacity. Calculate all residuals and the regional residual sum.

Graph dynamics

P6. Construct D, W, and L for a two-node graph of weight w.

P7. Find both Laplacian eigenvalues of that graph.

P8. For an isolated free node, solve the discrete update from $q^0 = 1$, $q^1 = 1.2$ for q^2, q^3.

P9. On a periodic chain, evaluate $\lambda(k)$ at $ka = 0, \pi/2, \pi$.

P10. For $d = 2$, $a = c = 1$, and $\Omega_0 = 0$, find the largest stable $\Delta\tau$.

Waves and nonlinearity

P11. With $a = c = 1$, $\Delta\tau = 0.5$, $\Omega_0 = 0$, and $k = \pi/2$, calculate ω from the exact one-dimensional dispersion relation.

P12. Expand $4\sin^2(ka/2)/a^2$ through order a^2.

P13. For $\Omega_0 = 3$, $\mu = 2$, $\lambda = 0.4$, and $A = 0.5$, estimate the Duffing frequency.

P14. A normalized mode is equal on four nodes and zero elsewhere. Calculate its participation ratio.

P15. Two matched gaps are $\omega_a = 5$ and $\omega_b = 2$. Calculate the mass ratio.

Gauge structure

P16. Show $D_{ij}\psi$ transforms with the phase at node i.

P17. For link phases $(0.2, 0.3, -0.1, -0.4)$ rad around a plaquette, calculate the plaquette phase.

P18. Expand $1 - \cos\Phi$ through fourth order.

P19. If two $U(1)$ fields have charges 2 and -1, determine the charge of their product.

P20. Explain in two sentences why a Feynman diagram requires a derived vertex coefficient.

Constants and evidence

P21. Show dimensionally that c^5/G is power.

P22. Compute the spherical area in units of ℓ_P^2 for radius $2\ell_P$.

P23. Use Equation (17.18) to find how the cross section changes if g doubles.

P24. If $y = x^3$, derive the linearized relative uncertainty $u(y)/|y|$ in terms of $u(x)/|x|$.

P25. A model uses a measured mass to choose a frequency scale and then returns that same mass. Classify the result.

P26. Write a three-way split of a 1,000-event dataset with 200 design events, 300 calibration events, and the remainder held out.

P27. For independent residuals $r = (1, -2, 1)$ with unit variances, calculate $\chi^2 = r^\mathsf{T} r$.

P28. A measured phase difference is 2.4 rad across 6 m. Find k.

P29. Sampling occurs every 0.002 s. Find the Nyquist frequency.

P30. State one numerical failure rule for a gauge-invariance unit test.

Research design

P31. Design a blind search for localized modes that avoids particle-mass tuning.

P32. Name the four maps needed to turn a deterministic micro-state into quantum outcome frequencies.

P33. State the CHSH local bound and the quantum maximum.

P34. Give one operational no-signalling equality.

P35. List the outputs required before a capacity field can be used in a cosmological likelihood.

D

Solutions

S1. $2\pi/0.25 = 8\pi \approx 25.13$ updates; a full crossing occurs between updates 25 and 26.
S2. $2000/20 = 100$ cycles.
S3. $\ln P = \ln 5 - 2\ln\sigma$, so $d_s = -2(-2) = 4$.
S4. The path through b costs $1 + 2 = 3$, less than direct cost 4; hence $d_G(a,c) = 3$.
S5. $r = (0.6, 0.1, 0)$ and the regional sum is 0.7.
S6. $D = \mathrm{diag}(w,w)$, $W = \left(\begin{smallmatrix} 0 & w \\ w & 0 \end{smallmatrix}\right)$, and $\mathsf{L} = \left(\begin{smallmatrix} w & -w \\ -w & w \end{smallmatrix}\right)$.
S7. The constant vector has eigenvalue 0; the antisymmetric vector has eigenvalue $2w$.
S8. Free motion has constant increment 0.2: $q^2 = 1.4$, $q^3 = 1.6$.
S9. Equation (7.10) gives 0, 2, and 4.
S10. Equation (10.3) gives $\Delta\tau^2(8) \le 4$, so $\Delta\tau \le 1/\sqrt{2}$.
S11. The right side is $4\sin^2(\pi/4) = 2$. Thus $16\sin^2(\omega/4) = 2$, giving $\omega = 4\arcsin(1/\sqrt{8}) \approx 1.445$.
S12. $4\sin^2(ka/2)/a^2 = k^2 - a^2k^4/12 + \mathcal{O}(a^4k^6)$.
S13. The correction is $3\lambda A^2/(8\mu\Omega_0^2) = 0.0020833$, so $\Omega \approx 3.00625$.
S14. Equal support on four nodes gives $P = 4$.
S15. $m_a/m_b = \omega_a/\omega_b = 2.5$.
S16. Direct substitution gives $D'_{ij}\psi' = \mathrm{e}^{\mathrm{i}q\alpha_i} D_{ij}\psi$.
S17. The oriented phase sum is $0.2 + 0.3 - 0.1 - 0.4 = 0$ rad, so $U_\square = 1$.
S18. $1 - \cos\Phi = \Phi^2/2 - \Phi^4/24 + \mathcal{O}(\Phi^6)$.
S19. Charges add: $2 + (-1) = 1$.
S20. The diagram is a term in an amplitude expansion. Its line types and vertex factor come from a normalized effective action, so without the coefficient it supplies no rate.
S21. $[c^5/G] = (L^5T^{-5})/(L^3M^{-1}T^{-2}) = ML^2T^{-3}$, the dimension of energy per time.
S22. $A = 4\pi(2\ell_P)^2 = 16\pi\ell_P^2$.
S23. $\sigma \propto g^2$, so doubling g multiplies σ by four.
S24. $u(y) \approx |3x^2|u(x)$, hence $u(y)/|y| \approx 3u(x)/|x|$.
S25. Calibration followed by identity/conversion, not a held-out prediction.
S26. $D_{\text{design}} = 200$, $D_{\text{cal}} = 300$, and $D_{\text{test}} = 500$ events, with disjoint identifiers.
S27. $\chi^2 = 1^2 + (-2)^2 + 1^2 = 6$.
S28. $k = 2.4/6 = 0.4\,\mathrm{rad.m}^{-1}$.
S29. $f_N = 1/(2 \times 0.002) = 250\,\mathrm{Hz}$.
S30. Example: fail if the relative change in the gauge-invariant link action exceeds 10^{-12} for any of 10,000 seeded random transformations.
S31. Fix the graph family, parameters, objective, localization statistic, continuation method, and stability threshold before viewing particle data; publish every stable dimensionless gap with multiplicity accounted for.
S32. Preparation $P \mapsto \mu_P$, deterministic evolution U, coarse state/observable map, and apparatus outcome response $A(a,\lambda)$.
S33. Local CHSH bound 2; quantum Tsirelson maximum $2\sqrt{2}$.
S34. $\sum_y P(x,y|a,b) = \sum_y P(x,y|a,b')$ for every x, a, b, b'.
S35. A derived coarse field normalization; action coefficients; source and response map; background solution; perturbation equations; initial conditions; calibration policy; and covariance-aware observable likelihood.

E

Equation and claim ledger

Equation	Object	Status	Primary dependency
(1.1)	Ordered history	DEFINED	Relational state space
(1.5)	Operational time	PROPOSED	Stable recurrent pattern
(2.1)	Pattern identity	DEFINED	Coarse map, tolerance, symmetry
(3.3)	Local capacity	PROPOSED	Nonnegative local demand
(8.1)	Scalar graph action	DEFINED	Fixed benchmark graph
(8.4)	Benchmark field equation	DERIVED	Variation of the action
(9.5)	Exact lattice spectrum	DERIVED	Plane-wave eigenmodes
(10.3)	Linear stability domain	DERIVED	Maximum lattice eigenvalue
(11.6)	Nonlinear frequency shift	DERIVED	Weak Duffing approximation
(12.8)	Link-action invariance	DERIVED	Local gauge transformation
(13.7)	Continuum operator target	PROPOSED	Coarse matching
(14.3)	Quantum probability target	MEASURED INPUT	Established quantum formalism
(14.5)	Bell–CHSH bound	TEST	Local measurement-independent model
(15.3)	Torsion geometry	DEFINED	Tetrad and connection
(16.1)	EQEF balance candidate	PROPOSED	Residual capacity current
(17.12)	Stefan–Boltzmann constant	DERIVED	Quantum radiation law and SI inputs
(21.4)	Collider counting likelihood	DEFINED	Poisson model and nuisance constraints

F

Author revision protocol

This protocol lets new ideas enter the book without breaking the dependency chain.

F.1 One-page proposal card

For every revision, complete:

1. **Name and version.**
2. **Layer:** foundation, benchmark, spectrum, gauge, capacity, quantum, gravity, cosmology, or evidence.
3. **Replaced object:** exact equation, definition, or map.
4. **New object:** full types, domains, units, parameters, boundary conditions, and tie-breaks.
5. **Reason:** inconsistency repaired or new explanatory role.
6. **Dependencies affected:** atlas codes and equation numbers.
7. **Checks:** algebra, dimensions, limits, symmetry, stability, conservation, code tests.
8. **Empirical policy:** design data, calibration data, held-out data, likelihood, and failure rule.

F.2 Promotion rules

- A metaphor becomes a DEFINED object when its mathematical type and measurement rule are explicit.
- A proposed equation becomes DERIVED only when it follows from earlier displayed assumptions.
- A model coefficient becomes matched when the calibration datum and uncertainty are recorded.
- A result becomes a prediction only after the relevant card is frozen and the comparison target is held out.

F.3 Consistency sweep

After a foundational change, rerun in order: notation/types, dimensions, deterministic closure, conservation, linear spectrum, stability, gauge tests, continuum scaling, pattern search, observable mapping, covariance, and held-out likelihood. Increment the edition number and retain the prior edition as provenance.

G

Glossary

Admissible set
States or state pairs satisfying every local constraint.

Benchmark
A deliberately limited model in which exact calculations can be performed.

Brillouin zone
The distinct wave-vector domain represented by a periodic lattice.

Calibration
Use of data to select a parameter, scale, or dictionary.

Capacity
The fixed maximum of a declared local transition demand.

Coarse-graining
A map that retains resolved large-scale information while averaging microscopic detail.

Covariance
A measure of how uncertainties in two quantities move together.

Dispersion relation
The relation between frequency and wave vector.

Effective field theory
An operator expansion organized by symmetry and scale.

Emergence
Construction of a stable higher-level description from lower-level dynamics.

EQEF
In this book, the ledger and possible coarse field of residual local transition capacity.

Gauge invariance
Independence of physical observables from local internal reference choices.

Graph Laplacian
The operator comparing each node value with its weighted neighbours.

Group velocity
The derivative $\partial\omega/\partial k$ governing a narrow packet's envelope motion.

Held-out test
Data not used to choose equations, cuts, priors, parameters, or units.

Holonomy
Net transporter obtained around a closed loop.

Identity
A relation true by definition or algebraic rearrangement.

Matching
Equating coefficients in two descriptions at a declared scale and convention.

Node
A relational degree of freedom in the benchmark or a persistent class in the emergent ontology.

No-signalling
Independence of a local observable marginal from a remote setting choice.

Operational clock
A robust recurrent pattern used to label duration.

Pattern
A persistent equivalence class under allowed transport, phase change, or relabeling.

Plaquette
An elementary oriented loop used to encode lattice curvature.

Prediction
A held-out observable calculated after the model and calibration are frozen.

Residual capacity
The fraction $1 - C_i$ remaining at a node after local demand is evaluated.

Spectral dimension
Scale-dependent dimension inferred from diffusion return probability.

Torsion
Geometric field strength describing infinitesimal transport nonclosure.

Update order
The primitive succession label n, distinguished from physical clock time.

H

Annotated bibliography and intellectual lineage

End Theory sits beside several established traditions: relational accounts of space and time, discrete dynamics, lattice gauge theory, nonlinear waves, effective field theory, quantum foundations, gravitation with and without torsion, cosmology, metrology, statistical inference, and complex-systems science. The references below credit the people and collaborations whose work defines those neighbouring subjects. Inclusion records relevance; it does not imply endorsement of End Theory.

Bibliography

Classical mechanics, space, time, and relativity

[1] I. Newton, *Philosophiæ Naturalis Principia Mathematica* (1687). The classical synthesis of motion and universal gravitation.

[2] G. W. Leibniz and S. Clarke, *The Leibniz–Clarke Correspondence* (1715–1716). A foundational exchange over relational and absolute accounts of space and time.

[3] J.-L. Lagrange, *Mécanique analytique* (1788). Systematic variational mechanics.

[4] W. R. Hamilton, "On a general method in dynamics," *Philosophical Transactions of the Royal Society* **124**, 247–308 (1834).

[5] E. Mach, *The Science of Mechanics* (1883). Influential critique of absolute space and inertia.

[6] A. Einstein, "On the electrodynamics of moving bodies," *Annalen der Physik* **17**, 891–921 (1905).

[7] H. Minkowski, "Space and time," address to the 80th Assembly of German Natural Scientists and Physicians (1908).

[8] A. Einstein, "The foundation of the general theory of relativity," *Annalen der Physik* **49**, 769–822 (1916).

[9] E. Noether, "Invariant variation problems," *Nachrichten von der Gesellschaft der Wissenschaften zu Göttingen*, 235–257 (1918). The symmetry–conservation theorem.

[10] H. Weyl, "Gravitation and electricity," *Sitzungsberichte der Königlich Preussischen Akademie der Wissenschaften*, 465–480 (1918). Early gauge-geometric unification.

[11] A. S. Eddington, *The Mathematical Theory of Relativity* (Cambridge University Press, 1923).

[12] J. A. Wheeler, "Information, physics, quantum: the search for links," in *Complexity, Entropy, and the Physics of Information* (Addison-Wesley, 1990). The "it from bit" programme.

[13] J. Barbour, *The End of Time* (Oxford University Press, 1999). A modern timeless/relational perspective.

[14] C. Rovelli, *Quantum Gravity* (Cambridge University Press, 2004). Relational observables and loop quantum gravity.

Discrete geometry, graphs, and emergent spacetime

[15] T. Regge, "General relativity without coordinates," *Nuovo Cimento* **19**, 558–571 (1961), doi:10.1007/BF02733251.

[16] R. Penrose, "Angular momentum: an approach to combinatorial space-time," in *Quantum Theory and Beyond* (Cambridge University Press, 1971). Spin-network origins.

[17] L. Bombelli, J. Lee, D. Meyer, and R. D. Sorkin, "Space-time as a causal set," *Physical Review Letters* **59**, 521–524 (1987), doi:10.1103/PhysRevLett.59.521.

[18] G. Brightwell and R. Gregory, "Structure of random discrete spacetime," *Physical Review Letters* **66**, 260–263 (1991).

[19] A. Ashtekar, “New variables for classical and quantum gravity,” *Physical Review Letters* **57**, 2244–2247 (1986).

[20] C. Rovelli and L. Smolin, “Discreteness of area and volume in quantum gravity,” *Nuclear Physics B* **442**, 593–622 (1995).

[21] J. Ambjørn, J. Jurkiewicz, and R. Loll, “Dynamically triangulating Lorentzian quantum gravity,” *Nuclear Physics B* **610**, 347–382 (2001).

[22] S. Carlip, “Dimension and dimensional reduction in quantum gravity,” *Classical and Quantum Gravity* **34**, 193001 (2017).

[23] F. R. K. Chung, *Spectral Graph Theory* (American Mathematical Society, 1997).

[24] B. Mohar, “The Laplacian spectrum of graphs,” in *Graph Theory, Combinatorics, and Applications* (Wiley, 1991).

[25] M. Kac, “Can one hear the shape of a drum?” *American Mathematical Monthly* **73**, 1–23 (1966). Spectra as geometric probes.

[26] R. R. Coifman and S. Lafon, “Diffusion maps,” *Applied and Computational Harmonic Analysis* **21**, 5–30 (2006).

[27] M. Belkin and P. Niyogi, “Laplacian eigenmaps for dimensionality reduction and data representation,” *Neural Computation* **15**, 1373–1396 (2003).

[28] E. H. Lieb and D. W. Robinson, “The finite group velocity of quantum spin systems,” *Communications in Mathematical Physics* **28**, 251–257 (1972), doi:10.1007/BF01645779.

Numerical dynamics and lattice field theory

[29] R. Courant, K. Friedrichs, and H. Lewy, “On the partial difference equations of mathematical physics,” *Mathematische Annalen* **100**, 32–74 (1928). The CFL stability condition.

[30] J. von Neumann and R. D. Richtmyer, “A method for the numerical calculation of hydrodynamic shocks,” *Journal of Applied Physics* **21**, 232–237 (1950).

[31] C. Størmer, “Sur les trajectoires des corpuscules electrises,” *Archives des Sciences Physiques et Naturelles* **24**, 5–18 (1907). Early centred integration associated with the Størmer method.

[32] L. Verlet, “Computer experiments on classical fluids. I. Thermodynamical properties of Lennard-Jones molecules,” *Physical Review* **159**, 98–103 (1967).

[33] K. G. Wilson, “Confinement of quarks,” *Physical Review D* **10**, 2445–2459 (1974), doi:10.1103/PhysRevD.10.2445.

[34] J. Kogut and L. Susskind, “Hamiltonian formulation of Wilson’s lattice gauge theories,” *Physical Review D* **11**, 395–408 (1975).

[35] J. B. Kogut, “An introduction to lattice gauge theory and spin systems,” *Reviews of Modern Physics* **51**, 659–713 (1979).

[36] M. Creutz, *Quarks, Gluons and Lattices* (Cambridge University Press, 1983).

[37] H. J. Rothe, *Lattice Gauge Theories: An Introduction*, 4th ed. (World Scientific, 2012).

[38] I. Montvay and G. Münster, *Quantum Fields on a Lattice* (Cambridge University Press, 1994).

[39] H. B. Nielsen and M. Ninomiya, "A no-go theorem for regularizing chiral fermions," *Physics Letters B* **105**, 219–223 (1981), doi:10.1016/0370-2693(81)91026-1.

[40] P. H. Ginsparg and K. G. Wilson, "A remnant of chiral symmetry on the lattice," *Physical Review D* **25**, 2649–2657 (1982).

[41] D. B. Kaplan, "A method for simulating chiral fermions on the lattice," *Physics Letters B* **288**, 342–347 (1992).

[42] H. Neuberger, "Exactly massless quarks on the lattice," *Physics Letters B* **417**, 141–144 (1998).

Nonlinear waves, solitons, and localization

[43] G. Duffing, *Erzwungene Schwingungen bei veränderlicher Eigenfrequenz* (Vieweg, 1918).

[44] E. Fermi, J. Pasta, S. Ulam, and M. Tsingou, "Studies of nonlinear problems," Los Alamos report LA-1940 (1955).

[45] D. J. Korteweg and G. de Vries, "On the change of form of long waves advancing in a rectangular canal," *Philosophical Magazine* **39**, 422–443 (1895).

[46] N. J. Zabusky and M. D. Kruskal, "Interaction of solitons in a collisionless plasma and the recurrence of initial states," *Physical Review Letters* **15**, 240–243 (1965).

[47] A. C. Scott, F. Y. F. Chu, and D. W. McLaughlin, "The soliton: a new concept in applied science," *Proceedings of the IEEE* **61**, 1443–1483 (1973).

[48] S. Aubry, "Breathers in nonlinear lattices: existence, linear stability and quantization," *Physica D* **103**, 201–250 (1997).

[49] S. Flach and C. R. Willis, "Discrete breathers," *Physics Reports* **295**, 181–264 (1998).

[50] R. S. MacKay and S. Aubry, "Proof of existence of breathers for time-reversible or Hamiltonian networks of weakly coupled oscillators," *Nonlinearity* **7**, 1623–1643 (1994).

[51] P. W. Anderson, "Absence of diffusion in certain random lattices," *Physical Review* **109**, 1492–1505 (1958).

Quantum theory, gauge fields, and effective theories

[52] M. Planck, "On the law of distribution of energy in the normal spectrum," *Annalen der Physik* **4**, 553–563 (1901).

[53] M. Born, "Zur Quantenmechanik der Stoßvorgänge," *Zeitschrift für Physik* **37**, 863–867 (1926). Statistical interpretation of the wavefunction.

[54] W. Heisenberg, "Quantum-theoretical reinterpretation of kinematic and mechanical relations," *Zeitschrift für Physik* **33**, 879–893 (1925).

[55] E. Schrödinger, "Quantization as an eigenvalue problem," *Annalen der Physik* **79**, 361–376 (1926).

[56] P. A. M. Dirac, "The quantum theory of the electron," *Proceedings of the Royal Society A* **117**, 610–624 (1928).

[57] S. Tomonaga, "On a relativistically invariant formulation of the quantum theory of wave fields," *Progress of Theoretical Physics* **1**, 27–42 (1946).

[58] J. Schwinger, "Quantum electrodynamics. I. A covariant formulation," *Physical Review* **74**, 1439–1461 (1948).

[59] R. P. Feynman, "Space-time approach to quantum electrodynamics," *Physical Review* **76**, 769–789 (1949).

[60] F. J. Dyson, "The radiation theories of Tomonaga, Schwinger, and Feynman," *Physical Review* **75**, 486–502 (1949).

[61] C. N. Yang and R. L. Mills, "Conservation of isotopic spin and isotopic gauge invariance," *Physical Review* **96**, 191–195 (1954).

[62] Y. Nambu and G. Jona-Lasinio, "Dynamical model of elementary particles based on an analogy with superconductivity," *Physical Review* **122**, 345–358 (1961).

[63] J. Goldstone, "Field theories with superconductor solutions," *Nuovo Cimento* **19**, 154–164 (1961).

[64] P. W. Higgs, "Broken symmetries and the masses of gauge bosons," *Physical Review Letters* **13**, 508–509 (1964).

[65] F. Englert and R. Brout, "Broken symmetry and the mass of gauge vector mesons," *Physical Review Letters* **13**, 321–323 (1964).

[66] S. L. Glashow, "Partial-symmetries of weak interactions," *Nuclear Physics* **22**, 579–588 (1961).

[67] S. Weinberg, "A model of leptons," *Physical Review Letters* **19**, 1264–1266 (1967).

[68] A. Salam, "Weak and electromagnetic interactions," in *Elementary Particle Theory* (Almqvist and Wiksell, 1968).

[69] D. J. Gross and F. Wilczek, "Ultraviolet behavior of non-Abelian gauge theories," *Physical Review Letters* **30**, 1343–1346 (1973).

[70] H. D. Politzer, "Reliable perturbative results for strong interactions?" *Physical Review Letters* **30**, 1346–1349 (1973).

[71] G. 't Hooft, "Renormalizable Lagrangians for massive Yang–Mills fields," *Nuclear Physics B* **35**, 167–188 (1971).

[72] K. G. Wilson, "Renormalization group and critical phenomena. I," *Physical Review B* **4**, 3174–3183 (1971).

[73] S. Weinberg, "Phenomenological Lagrangians," *Physica A* **96**, 327–340 (1979), doi:10.1016/0378-4371(79)90223-1.

[74] M. E. Peskin and D. V. Schroeder, *An Introduction to Quantum Field Theory* (Addison-Wesley, 1995).

[75] A. Zee, *Quantum Field Theory in a Nutshell*, 2nd ed. (Princeton University Press, 2010).

[76] R. P. Woodard, "The theorem of Ostrogradsky," *Scholarpedia* **10**, 32243 (2015), doi:10.4249/scholarpedia.32243.

Quantum foundations and measurement

[77] D. Bohm, “A suggested interpretation of the quantum theory in terms of hidden variables,” *Physical Review* **85**, 166–193 (1952).

[78] H. Everett III, “Relative state formulation of quantum mechanics,” *Reviews of Modern Physics* **29**, 454–462 (1957).

[79] J. S. Bell, “On the Einstein Podolsky Rosen paradox,” *Physics* **1**, 195–200 (1964), doi:10.1103/PhysicsPhysiqueFizika.1.195.

[80] S. Kochen and E. P. Specker, “The problem of hidden variables in quantum mechanics,” *Journal of Mathematics and Mechanics* **17**, 59–87 (1967).

[81] J. F. Clauser, M. A. Horne, A. Shimony, and R. A. Holt, “Proposed experiment to test local hidden-variable theories,” *Physical Review Letters* **23**, 880–884 (1969).

[82] A. M. Gleason, “Measures on the closed subspaces of a Hilbert space,” *Journal of Mathematics and Mechanics* **6**, 885–893 (1957).

[83] B. S. Cirel’son, “Quantum generalizations of Bell’s inequality,” *Letters in Mathematical Physics* **4**, 93–100 (1980).

[84] A. Aspect, J. Dalibard, and G. Roger, “Experimental test of Bell’s inequalities using time-varying analyzers,” *Physical Review Letters* **49**, 1804–1807 (1982).

[85] W. H. Zurek, “Decoherence, einselection, and the quantum origins of the classical,” *Reviews of Modern Physics* **75**, 715–775 (2003).

[86] B. Hensen *et al.*, “Loophole-free Bell inequality violation using electron spins separated by 1.3 kilometres,” *Nature* **526**, 682–686 (2015), doi:10.1038/nature15759.

[87] M. Giustina *et al.*, “Significant-loophole-free test of Bell’s theorem with entangled photons,” *Physical Review Letters* **115**, 250401 (2015).

[88] L. K. Shalm *et al.*, “Strong loophole-free test of local realism,” *Physical Review Letters* **115**, 250402 (2015).

[89] H. M. Wiseman, “The two Bell’s theorems of John Bell,” *Journal of Physics A* **47**, 424001 (2014).

Gravitation, torsion, black holes, and holography

[90] D. Hilbert, “The foundations of physics,” *Nachrichten von der Gesellschaft der Wissenschaften zu Göttingen*, 395–407 (1915).

[91] E. Cartan, “On a generalization of the notion of Riemann curvature and spaces with torsion,” *Comptes Rendus de l’Académie des Sciences* **174**, 593–595 (1922).

[92] D. W. Sciama, “The physical structure of general relativity,” *Reviews of Modern Physics* **36**, 463–469 (1964).

[93] T. W. B. Kibble, “Lorentz invariance and the gravitational field,” *Journal of Mathematical Physics* **2**, 212–221 (1961).

[94] F. W. Hehl, P. von der Heyde, G. D. Kerlick, and J. M. Nester, “General relativity with spin and torsion,” *Reviews of Modern Physics* **48**, 393–416 (1976), doi:10.1103/RevModPhys.48.393.

[95] R. M. Wald, *General Relativity* (University of Chicago Press, 1984).

[96] C. W. Misner, K. S. Thorne, and J. A. Wheeler, *Gravitation* (W. H. Freeman, 1973).

[97] S. M. Carroll, *Spacetime and Geometry* (Addison-Wesley, 2004).

[98] K. Schwarzschild, "On the gravitational field of a mass point according to Einstein's theory," *Sitzungsberichte der Königlich Preussischen Akademie der Wissenschaften*, 189–196 (1916).

[99] R. Penrose, "Gravitational collapse and space-time singularities," *Physical Review Letters* **14**, 57–59 (1965).

[100] J. D. Bekenstein, "Black holes and entropy," *Physical Review D* **7**, 2333–2346 (1973).

[101] S. W. Hawking, "Particle creation by black holes," *Communications in Mathematical Physics* **43**, 199–220 (1975).

[102] G. 't Hooft, "Dimensional reduction in quantum gravity," arXiv:gr-qc/9310026 (1993).

[103] L. Susskind, "The world as a hologram," *Journal of Mathematical Physics* **36**, 6377–6396 (1995).

[104] J. Maldacena, "The large-N limit of superconformal field theories and supergravity," *Advances in Theoretical and Mathematical Physics* **2**, 231–252 (1998).

Cosmology and gravitational waves

[105] A. Friedmann, "On the curvature of space," *Zeitschrift für Physik* **10**, 377–386 (1922).

[106] G. Lemaître, "A homogeneous universe of constant mass and increasing radius," *Annales de la Société Scientifique de Bruxelles* **47**, 49–59 (1927).

[107] E. Hubble, "A relation between distance and radial velocity among extra-galactic nebulae," *Proceedings of the National Academy of Sciences* **15**, 168–173 (1929).

[108] H. P. Robertson, "Kinematics and world-structure," *Astrophysical Journal* **82**, 284–301 (1935).

[109] A. G. Walker, "On Milne's theory of world-structure," *Proceedings of the London Mathematical Society* **42**, 90–127 (1937).

[110] A. G. Riess *et al.*, "Observational evidence from supernovae for an accelerating universe and a cosmological constant," *Astronomical Journal* **116**, 1009–1038 (1998).

[111] S. Perlmutter *et al.*, "Measurements of Ω and Λ from 42 high-redshift supernovae," *Astrophysical Journal* **517**, 565–586 (1999).

[112] Planck Collaboration, "Planck 2018 results. VI. Cosmological parameters," *Astronomy & Astrophysics* **641**, A6 (2020).

[113] B. P. Abbott *et al.* (LIGO Scientific Collaboration and Virgo Collaboration), "Observation of gravitational waves from a binary black hole merger," *Physical Review Letters* **116**, 061102 (2016).

[114] B. P. Abbott *et al.*, "Multi-messenger observations of a binary neutron star merger," *Astrophysical Journal Letters* **848**, L12 (2017).

[115] S. Weinberg, *Cosmology* (Oxford University Press, 2008).

[116] P. J. E. Peebles, *Principles of Physical Cosmology* (Princeton University Press, 1993).

Particle data, collider measurements, and open data

[117] F. Takahashi *et al.* (Particle Data Group), "Review of Particle Physics," *International Journal of Modern Physics A* **41**, 2630011 (2026).

[118] ATLAS Collaboration, "Observation of a new particle in the search for the Standard Model Higgs boson with the ATLAS detector at the LHC," *Physics Letters B* **716**, 1–29 (2012).

[119] CMS Collaboration, "Observation of a new boson at a mass of 125 GeV with the CMS experiment at the LHC," *Physics Letters B* **716**, 30–61 (2012).

[120] ATLAS Collaboration, "ATLAS 13 TeV samples collection: at least four leptons," CERN Open Data record 15005 (2020), doi:10.7483/OPENDATA.ATLAS.2Y1T.TLGL.

[121] ATLAS Collaboration, "ATLAS 13 TeV samples collection: gamma–gamma," CERN Open Data record 15006 (2020).

[122] CERN, *CERN Open Data Portal*, opendata.cern.ch. Public datasets, software environments, and educational resources.

[123] E. Maguire, L. Heinrich, and G. Watt, "HEPData: a repository for high energy physics data," *Journal of Physics: Conference Series* **898**, 102006 (2017).

[124] G. Cowan, K. Cranmer, E. Gross, and O. Vitells, "Asymptotic formulae for likelihood-based tests of new physics," *European Physical Journal C* **71**, 1554 (2011).

Constants, thermodynamics, and metrology

[125] L. Boltzmann, "On the relation between the second law of the mechanical theory of heat and probability calculations," *Wiener Berichte* **76**, 373–435 (1877).

[126] J. Stefan, "On the relation between thermal radiation and temperature," *Sitzungsberichte der Kaiserlichen Akademie der Wissenschaften* **79**, 391–428 (1879).

[127] W. Wien, "A new relation of the radiation of black bodies to the second law of thermodynamics," *Sitzungsberichte der Königlich Preussischen Akademie der Wissenschaften*, 55–62 (1893).

[128] N. Bohr, "On the constitution of atoms and molecules," *Philosophical Magazine* **26**, 1–25 (1913).

[129] P. J. Mohr, D. B. Newell, B. N. Taylor, and E. Tiesinga, "CODATA recommended values of the fundamental physical constants: 2022," *Journal of Physical and Chemical Reference Data* **54**, 033105 (2025), doi:10.1063/5.0279860.

[130] Bureau International des Poids et Mesures, *The International System of Units (SI Brochure)*, 9th ed., version 4.01 (2025), doi:10.59161/AUEZ1291.

[131] National Institute of Standards and Technology, *Fundamental Physical Constants: 2022 CODATA Adjustment*, Standard Reference Database 121.

Inference, reproducibility, and model criticism

[132] T. Bayes, “An essay towards solving a problem in the doctrine of chances,” *Philosophical Transactions of the Royal Society* **53**, 370–418 (1763).

[133] R. A. Fisher, “On the mathematical foundations of theoretical statistics,” *Philosophical Transactions of the Royal Society A* **222**, 309–368 (1922).

[134] J. Neyman and E. S. Pearson, “On the problem of the most efficient tests of statistical hypotheses,” *Philosophical Transactions of the Royal Society A* **231**, 289–337 (1933).

[135] S. S. Wilks, “The large-sample distribution of the likelihood ratio,” *Annals of Mathematical Statistics* **9**, 60–62 (1938).

[136] H. Akaike, “A new look at the statistical model identification,” *IEEE Transactions on Automatic Control* **19**, 716–723 (1974).

[137] G. E. P. Box, “Science and statistics,” *Journal of the American Statistical Association* **71**, 791–799 (1976).

[138] R. D. Peng, “Reproducible research in computational science,” *Science* **334**, 1226–1227 (2011).

[139] M. D. Wilkinson *et al.*, “The FAIR guiding principles for scientific data management and stewardship,” *Scientific Data* **3**, 160018 (2016).

[140] B. A. Nosek *et al.*, “Promoting an open research culture,” *Science* **348**, 1422–1425 (2015).

Information, feedback, synchronization, and adaptive systems

[141] C. E. Shannon, “A mathematical theory of communication,” *Bell System Technical Journal* **27**, 379–423 and 623–656 (1948).

[142] N. Wiener, *Cybernetics: Or Control and Communication in the Animal and the Machine* (MIT Press, 1948).

[143] W. R. Ashby, *An Introduction to Cybernetics* (Chapman & Hall, 1956).

[144] A. M. Turing, “The chemical basis of morphogenesis,” *Philosophical Transactions of the Royal Society B* **237**, 37–72 (1952).

[145] I. Prigogine, *Self-Organization in Nonequilibrium Systems* (Wiley, 1977).

[146] Y. Kuramoto, “Self-entrainment of a population of coupled nonlinear oscillators,” in *International Symposium on Mathematical Problems in Theoretical Physics* (Springer, 1975).

[147] J. J. Hopfield, “Neural networks and physical systems with emergent collective computational abilities,” *Proceedings of the National Academy of Sciences* **79**, 2554–2558 (1982).

[148] G. Tononi, “An information integration theory of consciousness,” *BMC Neuroscience* **5**, 42 (2004).

[149] K. Friston, “The free-energy principle: a unified brain theory?” *Nature Reviews Neuroscience* **11**, 127–138 (2010).

[150] A. K. Seth and T. Bayne, “Theories of consciousness,” *Nature Reviews Neuroscience* **23**, 439–452 (2022). A comparative review of operational proposals.

Subject Index

Closing perspective

End Theory begins with a modest object: an ordered local change. Its ambition lies in the succession of constructions that follow. Repeated change must make clocks. Persistence must make identity. Stable influence must make neighbourhood. Long waves must make fields. Invariant loops must make gauge information. Local capacity must make a distinctive nonlinear response. A detector map must finally turn all of that mathematics into a number that nature can accept or reject.

The framework earns strength one explicit bridge at a time. The reader now has the equations, worked checks, status labels, computational tests, and research gates needed to follow those bridges in order.